International Journal of Nanoelectronics and Materials
IJNeaM
ISSN 1985-5761 | E-ISSN 2232-1535

Nickel recovery from treated nickel sludge by cyclic voltammetry under varying cathode materials in an electrowinning bath

Nurul Zufarhana Zulkurnai [a], Cheah Hoong Li [a], Umi Fazara Md Ali [a,b] *, Obid Tursunov [c,d], Subash C.B Gopinath [e,f], Naimah Ibrahim [g,h]

[a]*Faculty of Chemical Engineering Technology, Universiti Malaysia Perlis (UniMAP), 02600 Arau, Perlis, Malaysia*
[b]*Biomass Utilization Organization, Centre of Excellence (CoEBU), Universiti Malaysia Perlis (UniMAP), 02600 Arau, Perlis, Malaysia*
[c]*Department of Power Supply and Renewable Energy Sources, National Research University TIIAME, 39 Kari Niyazov, 100000 Tashkent, Uzbekistan*
[d]*Bioenergy and Environment Science & Technology Laboratory, College of Engineering, China Agricultural University, Beijing 100083, P. R. China*
[e]*Center for Global Health Research, Saveetha Medical College & Hospital, Saveetha Institute of Medical and Technical Sciences (SIMATS), Thandalam, Chennai – 602 105, Tamil Nadu, India*
[f]*Department of Technical Sciences, Western Caspian University, Baku AZ 1075, Azerbaijan*
[g]*Institute of Nano Electronic Engineering and 7Faculty of Civil Engineering Technology, Universiti Malaysia Perlis (UniMAP), 02600 Arau, Perlis, Malaysia*
[h]*Center for Separation Science & Technology (CSST), Department of Chemical Engineering, Faculty of Engineering, Universiti Malaya, Kuala Lumpur, Malaysia*
** Corresponding author. Tel.: +6019-5747680; e-mail: umifazara@unimap.edu.my*

Received 08 May 2025, Revised 16 May 2025, Accepted 19 May 2025

ABSTRACT

Nickel is famous for being the electroplating element due to its corrosion resistance. However, after a certain period of time, the nickel electroplating solution needs to be disposed of, but the disposal cost is expensive. Thus, electrowinning is preferred instead of disposing of the electrowon nickel ions out of the sludge from the electroplating solution. This study aimed to evaluate electrowinning parameters that maximize nickel recovery from treated nickel sludge using the ideal commercial cathode material type for kinetic studies. During the study, determination of the best cathode material type, optimization by using Design of Experiment (DOE)-Box-Bhenken Design on applied potential, pH, and contact time, and characterization of cathodes' surface morphology with deposited nickel have been conducted. Results show that graphite cathode recovered 56.74% followed by nickel metal (55.90%) and AISI 304 stainless steel (50.66%) at expected optimal electrowinning conditions of pH 5, 0.5 V and 3 hours. However, nickel deposits on graphite contain impurities and are difficult to extract. Thus, after considering commercialization aspects in the Analytical Hierarchy Process and the Technique for Order of Preference by Similarity to Ideal Solution (AHP-TOPSIS), the nickel cathode is the best. The optimal electrowinning conditions by using DOE are pH 6, 0.5 V and 1 hour with a maximum nickel recovery of 70.18%. The morphological characterization evidenced smooth, polycrystalline surfaces that become altered as the Ni grains increase. The electrochemical process has been discussed based on Nernst, Tafel, Anson and Butler Volmer equations. Overall, the nickel cathode has demonstrated significant potential as an ideal commercial cathode for nickel recovery.

Keywords: *Cyclic voltammetry; Electrowinning; Box-Behnken design; Nickel sludge; Cathodes*

1. INTRODUCTION

Currently, nickel is widely used in various industrial applications due to its characteristics, including corrosion resistance, high-temperature stability, strength, ductility, toughness, recyclability, catalytic and electromagnetic properties, till it can be thought of as a staple ingredient in products, showing its international importance. According to Nickel Institute [1], the first use of nickel is mainly used in stainless steel sector (65%), followed by batteries sector (17%), nickel-based alloys sector (5%), plating sector (5%), alloy steels sector (3%), stainless steel foundries sector (1%), nickel-based alloy foundries sector (1%), and other sectors (2%). Nickel is also used in a wide range of end-use sectors, which are consumer goods, catering and food processing sector (29%), followed by mobility and transport sector (25%), process industries (14%), architecture, building and construction sectors (12%), energy sector (12%), industrial components (5%), and other sectors (4%) [1]. The annual demand for nickel is 3,200,000 tons in 2022, according to the International Energy Agency (2023) [2] and is estimated to increase exponentially in the coming years to be utilized in these industries, which raises a signal of urgency due to the depletion of international nickel supply at a faster rate. Thus, nickel recovery from potential nickel-rich sources, other than mining the Earth, is vital to ensure the continuation of nickel supply to support the international demand, that act as a preventive strategy for nickel, being an Earth element that requires a long time to form.

This study focuses on the nickel recovery from the electronics industry, where the nickel obtained from the recovery process has a potential supply in sustainable fields, such as the automotive field, to become a part of the raw material to produce electric vehicles (EV) nickel–metal hydride batteries [3]. In addition, the nickel recovery product can also be used as a part of a stainless-steel component [4]. In the electronics industry, nickel is often used to electroplate their products for aesthetic appearance and its favorable properties, such as solderability and corrosion resistance. There are a few types of nickel solutions used in the nickel plating, such as sulfamate nickel bath, electroless nickel bath and Watts Bath. However, the common types of nickel used by industries are Watts Bath [5]. After a certain time of usage, the solution has become waste that is required to be disposed, which is costly. This is because the process of treating the sludge effectively requires various processes, such as neutralization and landfilling, where some processes are not that effective, like poor dewatering and sedimentation processes, which are a hassle and expensive [6, 7]. Due to that, the action of disposing of nickel sludge is potentially harmful to the environment and living organisms indirectly due to possible leaching of nickel and exposure, as well as costing money to do so. Furthermore, a reliable and cost-effective stabilization process after treatment is still lacking because, by far, the processes found at lab scale, such as cryogenic and solution discharging processes, are too costly to scale up industrially [8]. In addition, it is not sustainable to just dispose of treated waste, which is a waste of nickel resources. Thus, it is best to sustainably recover nickel through electrowinning, as it has efficient recovery of Ni^{2+} with minimal reagent and energy utilization as well as high nickel selectivity, which leads to high purity of nickel, compared to other recovery methods such as adsorption, chemical precipitation, and ion exchange [9].

Electrowinning is a process that uses the electrochemical system to deposit metal (nickel) to the cathode from the electrolyte (treated nickel sludge in this case) using electricity. This method is also easier to scale up to be utilized industrially compared to other methods. Since electrowinning can be done using 2 dimensional (2D) or 3 dimensional (3D) electrodes, this study uses 2D electrodes as it is works better for high concentration conditions stated by Md Ali [10] because 3D electrodes, such as fluidized bed cell, easily get clogged and obtain mechanical problems due to high metal deposited on its pores since it is porous outside. Through this method, companies can save on disposal costs and gain nickel resources as added value to the company, making it another business line to sell recovered nickel to other industries. On the other hand, by conducting recovery through the electrowinning process, the impact of nickel waste on the environment and living organisms can also be reduced. Therefore, this study is initiated to ensure maximum nickel recovery by the electrowinning method for commercialization by discovering the best cathode material type together with its optimal electrowinning conditions using treated nickel sludge as the electrowon bath. This research has high scientific value due to its potential impact in solving nickel depletion and environmental issues, prolonging nickel utilization in products having utmost quality and performance, and providing more exploration into electrowinning using potential influencing factors and kinetic studies.

Table 1 summarizes the past studies by the researchers from 2019 until 2023, on the cathode material types used with their optimal operating conditions for maximum yield of Ni. Some of the material types used as cathodes in nickel baths are stainless steel, aluminium, titanium, copper, gold, and graphite. Nickel metal cathodes in the pure state receive little interest among researchers; only a few studies are done using composite or alloy forms, such as the study by Baraniak *et al.* [11] using nickel cobalt (NiCo) foam. Thus, the study of electrowinning using a nickel cathode is considered scarce, making it the novelty of this research. The comparison among types of materials (nickel, graphite and AISI 304 stainless steel) plus insights into factors of nickel recovery with kinetic studies and optimization further adds to the originality of the research. This research also challenges the popular cathode choice in industrial electrowinning, which is stainless steel [12], to be proven as the true best cathode material by using it as the control in this experiment.

Table 1. Summary of related studies on the cathode material types

Cathode material types	Reference	Optimal operating conditions for Ni^{2+} electrodeposition and recovery
Stainless Steel	[13]	400 A/m^2, 55°C and pH 5
	[14]	pH 2, 3.5 V, 1.5 A/dm^2, 24 hours, 200 rpm, ambient temperature
	[15]	60 minutes, pH 2.1, 25°C
	[16]	pH 4, 120 minutes, –1 mA/cm^2
	[17]	2.2 V, 9 hours, pH 3, 50 mL/min
	[18]	40 minutes, pH 7, 90–100°C, 125 A/m^2
Aluminium	[19]	pH 5, 70°C, 6 V, 3 hours (with sludge impurities)
Graphite	[20]	1500°C, 1.04 hours, 1.5 A/cm^2, inert atmosphere with argon flowrate of 400 sccm
Nickel	Lack of study	-
Titanium	[21]	120 A/m^2, pH 3.5–4.1, 45–55°C, additives (H_3BO_3 30g/L, saccharin 1.5 g/L)
	[22]	pH 3, 60°C, 220 A/m^2, 2 hours, (>1250 mg/L aluminium ion (Al^{3+}))
Copper	[23]	6 mA/dm^2, pH 3, 10 minutes
Gold	[24]	pH 3–5, 7 hours, 50–60 mA/m^2

2. MATERIALS AND METHODS

2.1. Chemicals and Materials

Materials used in the experiment were steel wires, platinum mesh, 100% nickel plates, graphite plates, and AISI 304 stainless steel plates with 0.1 mm thickness, respectively purchased from a local retailer (Malaysia). The chemicals required in this experiment were nickel sulphate hexahydrate, (98.5%, Bendosen Laboratory Chemicals, Kuala Lumpur, Malaysia), nickel (II) chloride 6-hydrate, (Pure, HmbG Chemicals, Kuala Lumpur, Malaysia), boric acid, (99.5%, Sigma-Aldrich, St. Louis, MO, USA), sulphuric acid, (96–98%, Thermo Fisher Scientific, Kuala Lumpur, Malaysia), and sodium hydroxide, (98%, HmbG Chemicals, Kuala Lumpur, Malaysia). All chemicals used in this study were of analytical grade.

2.2. Instruments

The instruments included in the experiment are a stirring hotplate, LMS-1003, and a magnetic bar from Daihan Labtech (Indonesia) to dissolve the treated nickel sludge with sulphuric acid into a homogeneous solution. The inductively coupled plasma optical emission spectrophotometer (ICP-OES) Optima 8000 from Perkin Elmer (USA) was used to measure the composition and concentration of treated nickel sludge, and the analytical balance BS244S from Sartorius was used to weigh treated nickel sludge. For measuring the pH of the treated nickel sludge, the MW100 PRO pH meter from Milwaukee (Romania) has been used. The scanning electron microscope (SEM) TM 3030 Plus from Hitachi (Japan) with energy dispersive X-ray spectrophotometer (EDX) EDAX Octane Elite with ApEX software from AMETEK (USA) was used to analyze the characterization of cathodes' surface morphology. The standard glass calomel electrode HI5412 from Hanna Instruments (Italy) was used as a reference electrode, the automatic voltage stabilizer AVS1000-3UK from Neuropower (Malaysia) was used to regulate the power supply to the potentiostat, and the potentiostat/galvanostat PGSTAT204 with Nova 2.1.7 software from Metrohm Autolab (Malaysia) was used to fix and measure the electrical potential in the experiment.

2.3. Preparation of Simulated Watts Electrolyte Type

During the preparation of simulated Watts electrolyte type, 300 g/L of nickel sulphate, 40 g/L of nickel chloride and 30 g/L of boric acid were added into the beaker containing 1 L of distilled water. The beaker containing the solution was placed on the hot plate and heated to a temperature of 55°C. During the heating process, the magnetic stirrer was used to stir the solution until all the solids inside the solution were diluted and homogenized.

2.4. Preparation of Treated Nickel Sludge

The precipitation process was first done by adjusting the pH of the simulated Watts electrolyte type to pH 13 by adding 2 M of sodium hydroxide to the simulated Watts Electrolyte Type. After the desired pH was obtained, the solution was left to stir for 6 hours with 350 rpm applied for homogenization purposes. Then, the nickel precipitate form was filtered from the solution and dried in the oven at a temperature of 120°C for 4 hours to completely remove the moisture.

2.5. Preparation of Treated Nickel Solution

Treated nickel sludge was leached by adding 1.5 M sulphuric acid in a ratio of 1:10 using a hotplate and magnetic stirrer at 960 rpm until all sludge dissolved at room temperature and atmospheric pressure. For the optimization process of electrowinning, the desired pH of the electrolyte has been adjusted by using 1.5 M sulphuric acid and 2 M sodium hydroxide. The prepared electrolytes are left to cool before the experiment. The final concentration of Ni in the treated nickel solution is 10.077 g/L.

2.6. Preparation of the Electrode

A nickel plate was cut into sizes of 2 cm by 2 cm using a metal cutter, with a hole made at the top using a hammer and nail to twirl a steel wire through the hole and weighed on a beaker using an analytical balance and placed as the working electrode (cathode). This preparation is repeated for AISI 304 stainless steel and graphite plates.

2.7. Selection of the Ideal Commercial Cathode Material Type

Each type of flat plate cathode material was tested in electrolyte containing 99.80% Ni^{2+} and 0.20% supporting ions by using pH 5, 0.5 V and 3 hours of contact time at ambient conditions (room temperature and standard atmospheric pressure) on the potentiostat by using the Nova 2.1.7 software for cyclic voltammetry, linear voltammetry and chronoamperometry analysis with scan rate set to 0.2 $V \cdot s^{-1}$. After that, the final weight of each cathode material type with nickel deposited was taken for calculations of current efficiency. The Ni recovery by each cathode material was calculated using the initial and final concentrations of nickel ions (Ni^{2+}) in samples of electrolyte measured using the ICP-OES. After the electrowinning process for each cathode material type was completed, the cathodes were taken for characterization analysis by using electron microscopy–energy dispersive X-ray (SEM-EDX) analysis. With all the data obtained from the experiment and research, the combination of the Analytical Hierarchy Process and the Technique for Order of Preference by Similarity to Ideal Solution (AHP-TOPSIS) selection method, using Super Decisions and Decision Radar software, was used to determine the ideal commercial cathode material type using certain factors with their respective weightages [25, 26].

2.8. Cyclic Voltammetry Analysis

Cyclic voltammetry analysis is carried out on the treated solution in an electrochemical cell fitted with a flat plate working electrode (cathode), reference electrode (standard calomel electrode 3.5 M) and counter electrode (anode

using platinum mesh) that are connected to a potentiostat for voltage supply. The working and counter electrodes are ensured to be immersed two-thirds into the electrowon bath for proper nickel deposition. The experiment was done for nickel, AISI 304 stainless steel and graphite as working electrodes, respectively. The operating conditions of voltage and time are controlled and monitored by the measurements taken from the reference electrode connected to the potentiostat and software, whereas the pH is measured and adjusted to its pH setpoint using acid and/or alkali depending on the reading of the pH meter. The experiment was done in an air-conditioned laboratory to ensure consistent room temperature, where the temperature of the electrolyte is constantly measured and adjusted to room temperature using a hot or cold-water bath.

2.9. Electrowinning Parameter Optimization Analysis

In the electrowinning process, parameters of pH (A), contact time (B) and applied potential (C) have been optimized by using Design of Experiment (DOE) that utilizes statistics and other mathematical techniques to obtain maximum nickel recovery, tested using ICP-OES as the response through the experimental method used in cyclic voltammetry analysis. The ranges of pH, electrical potential and contact time are pH 4 to pH 6, 0.5 V to 0.6 V, and 1 hour to 3 hours, respectively. Table 2 shows the optimized conditions for the electrowinning process set by the Box-Behnken Design, a type of response surface methodology in DOE.

2.10. Characterization Analysis

The surface morphology of nickel electrodeposited at the cathodes was observed by using SEM and EDX analysis to determine the elements of the deposit at the cathode.

Table 2. Optimized conditions for the electrowinning process

Run	Parameter		
	pH	Contact Time (hour)	Applied Potential (V)
1	4	3	0.55
2	6	2	0.6
3	5	2	0.55
4	6	3	0.55
5	6	1	0.55
6	5	1	0.5
7	4	2	0.6
8	5	2	0.55
9	4	2	0.5
10	5	3	0.6
11	5	3	0.5
12	5	2	0.55
13	4	1	0.55
14	6	2	0.5
15	5	1	0.6
16	5	2	0.55
17	5	2	0.55

2.11. Kinetic Study

After the experiment was completed for finding the ideal commercial cathode material type with its optimized electrowinning parameters, kinetic models were discovered to show the interaction between Ni^{2+} and cathode material type together with the optimal conditions for maximum nickel recovery using Nerst equation, Anson equation, Tafel equation and Butler-Volmer equation shown in Equations (1), (2), (3) and (4), respectively through voltammetries and chronoamperometry.

$$E = E_f^0 - \frac{2.303\ RT}{nF}\log\left(\frac{[Ni^{2+}]}{[Ni]}\right) \quad (1)$$

$$Q = \frac{2nFAC\ (Dt)^{0.5}}{\pi^{0.5}} + Q_{dl} + Q_{ads} \quad (2)$$

$$i = i_o\left[\exp\left(\frac{\propto_a F\left(E - E_{eq}\right)}{RT}\right) - \exp\left(\frac{-\propto_c F\left(E - E_{eq}\right)}{RT}\right)\right] \quad (3)$$

$$\eta = -\frac{2.303\ RT}{\alpha_c F}\log\frac{|i|}{i_o} \quad (4)$$

The Nernst equation (Equation (1)) is used to understand the equilibrium potential of the half reaction under non-standard conditions, as stated by Compton *et al.* [27] and Zhang *et al.* [12], where E is the equilibrium potential for Ni^{2+} half-cell reaction versus the reference electrode potential, E_f^0 is the formal potential, R is the universal gas constant, T is the temperature, n is the valency and F is the Faraday's constant, which can be obtained from the voltammetries. The chronoamperometry was related to the Anson equation (Equation (2)) for charge to see the oxidation and reduction reactions occurring at that time, where Q_{dl} is the double layer charge, Q_{ads} is the Faradaic Ni^{2+} charge, C is substrate concentration, A is active area of working electrode, t is time, and D is diffusion coefficient [28]. Butler-Volmer and Tafel equations (Equations (3) and (4)) were also relevant as electrode kinetics for measuring the current density against the overpotential in redox reaction between Ni^{2+} and Ni using both voltammetry and chronoamperometry [29]. For Equation (3), i is the current density (I/A), i_o is the equilibrium exchange current density at E_{eq}, and $\propto_a$ and $\propto_c$ are the charge transfer coefficients at the anode and cathode, respectively [28]. For Equation (4), η is the overpotential, α_c is the charge transfer coefficient at the cathode, i is the current density and i_o is the equilibrium exchange current density [28].

3. RESULTS AND DISCUSSION

3.1. Determination of Ideal Commercial Cathode Material Type

From Figure 1, based on Ni^{2+} concentration in the electrolyte samples analysed by the ICP-OES, graphite turns out to recover the most Ni^{2+} (56.74%) compared to nickel (55.90%) and AISI 304 stainless steel (50.66%) under operating conditions of 0.5 V, pH 5, and 3 hours of contact time at ambient conditions (room temperature and

standard atmospheric pressure) using the electrolyte containing 99.80% Ni^{2+} and 0.20% supporting ions. Then, calculations based on the weight of deposited nickel on cathodes show that graphite have highest current efficiency of 39.57%, followed by nickel (24.35%) and AISI 304 stainless steel (6.09%), which proves that the current efficiency of materials is proportional to nickel recovery. However, the SEM and EDX analysis shows that dendrite nickel crystals deposited on the evenly distributed microporous rough surfaced graphite cathode in a hierarchical manner, stated by López-Mata *et al.* [28] and Zulkurnai *et al.* [30], is 6.2% w/w, lesser than that of nickel cathodes having discontinuous multicrystalline layers with grains and its boundaries of nickel (100% w/w) stated by Leiva-García *et al.* [31] and Peshcherova *et al.* [32], plus having impurities with sodium crystals (24.7% w/w) in its deposition when comparing Figure 2 (a) and (b). AISI 304 stainless steel cathode in Figure 2 (c) having a smooth layer of small grain sizes with an extensive grain boundary network, which accelerates the formation of the oxide layer, as stated by Gupta & Srivastava [33] is the least (1.3% w/w), which is aligned with the results of nickel recovery and current efficiency. There is a good protective film on the cathodes in Figure 2 (a), (b), and (c) [34]. The rest of the elements in the EDX analysis that are not mentioned are part of the material construction of the cathodes.

The main reason that the graphite cathode has a higher nickel recovery than the nickel cathode is that the construction of the graphite cathode, which is an edge plane pyrolytic graphite, is full of pores, as the rough surface has a random array of highly ordered microband electrodes, as stated by Compton *et al.* [27], shown in Figure 2 (b). The edge plane of the graphite cathode that has surface defects that expose its edges due to cuts is primarily the site of electrodeposition for fast and reversible kinetics, rather than the basal plane, which is inert, characterized by its very smooth surface, as shown in Figure 3 (d). This is shown from observation when the graphite cathode releases a lot of water after it is taken out. Although the graphite cathode is holding a lot of nickel ions, the nickel deposited within the cathode in scattering positions and unable to be recovered properly for commercial purpose (which require further processing for extraction), due to the disappearance of nickel and still having water retention despite being dried already has proven and shown practically in the sequence of Figure 3 (a), (b) and (c). It is done with 3.5 V since the experiment with 0.5 V is not that visible, as shown in Figure 3 (d). In addition, the reduction reaction of hydrogen is focused more on the graphite cathode rather than the reduction of nickel, since graphite is a non-metal, with proof of corrosion stains of the wire hole on the cathodes shown in Figures 3 (a), (b) and (c). Thus, the graphite cathode is holding more nickel ions, but not deposited, making the graphite cathode itself invalid for the selection of the ideal commercial cathode material type as it does not achieve the purpose of this study.

Furthermore, sodium impurities are deposited because they act as supporting ions to bring along Ni^{2+} for deposition, as stated by Compton *et al.* [27], since graphite is a non-metal that does not sufficiently conduct electricity

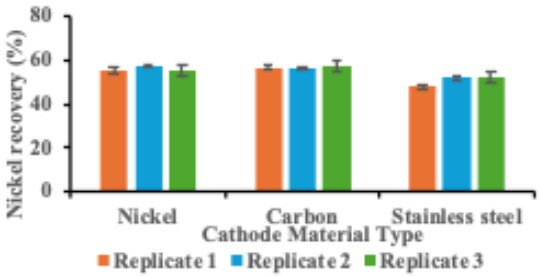

Figure 1. Comparison of cathode material type on nickel recovery

(a)

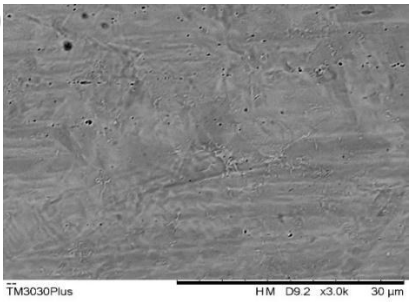

Element	Weight %	MDL	Atomic %	Error %
Nickel | New Sample | Area 7 | Selected Area 1				
Ni K	100.0	0.76	100.0	3.7

(b)

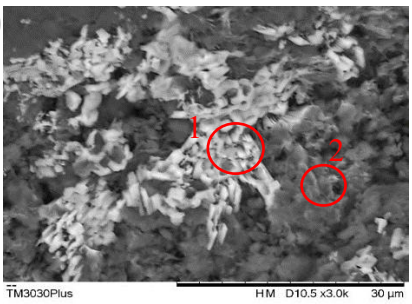

Element	Weight %	MDL	Atomic %	Error %
Nickel | New Sample | Area 10 | Selected Area 1				
C K	54.2	0.31	66.1	11.8
O K	22.9	0.24	20.9	12.3
Na K	15.5	0.27	9.9	10.4
S K	6.0	0.14	2.7	5.5
Ni K	1.5	0.49	0.4	21.2
Nickel | New Sample | Area 10 | Selected Area 2				
C K	20.2	0.58	30.6	13.4
O K	35.9	0.16	40.7	11.2
Na K	24.7	0.24	19.5	10.5
S K	12.9	0.12	7.3	5.7
Ni K	6.2	0.43	1.9	7.4

(c)

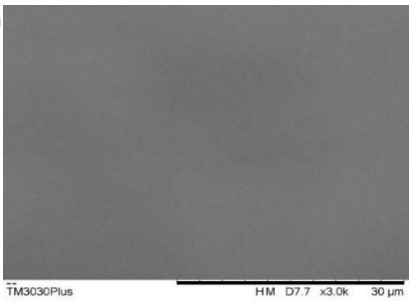

Element	Weight %	MDL	Atomic %	Error %
Nickel | New Sample | Area 3 | Selected Area 1				
Si K	1.7	0.21	3.2	13.2
Cr K	13.1	0.32	13.7	5.4
Mn K	10.2	0.62	10.1	5.5
Fe K	72.1	0.84	70.3	3.7
Ni K	1.3	0.72	1.2	37.5
Cu K	1.7	0.91	1.4	31.4

Figure 2. SEM and EDX analysis for (a) nickel, (b) graphite, and (c) AISI 304 stainless steel in electrolyte from treated nickel sludge

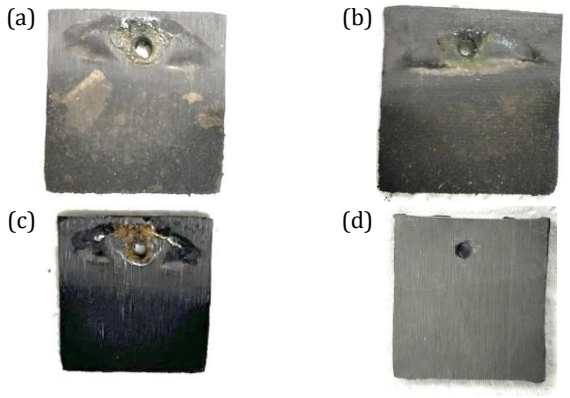

Figure 3. Graphite cathode after experiment with 3.5 V, where (a) nickel deposits are seen scattered, then (b) some nickel deposits disappeared, and (c) all disappeared and still moist (the darker shade) after several hours, even after drying, whereas (d) is done with 0.5 V

compared to nickel and AISI 304 stainless steel electrodes [35]. In addition, the reduction reaction of hydrogen is focused more on the graphite cathode rather than the reduction of nickel, since graphite is a non-metal. Thus, the graphite cathode is holding more nickel ions, but not deposited, making the graphite cathode itself invalid for the selection of the ideal commercial cathode material type as it does not achieve the purpose of this study.

To determine the best cathode material, considerations of other factors are also required for commercialization purposes through the Analytical Hierarchy Process and the Technique for Order of Preference by Similarity to Ideal Solution (AHP-TOPSIS) analysis method using data obtained from experiment and research. The electrical resistivity data of nickel, AISI 304 stainless steel, and graphite are 6.84×10^{-8} Ω·m by Karimzadeh *et al.* [36], 7.20×10^{-7} Ω·m by Ismon *et al.* [37] and 4.00×10^{-6} Ω·m by Jäger & Frohs [38], respectively. The material availability of nickel, AISI 304 stainless steel, and graphite is based on 2021, which are 2.69×10^{6} tonnes stated by Jaganmohan [39], 6.14×10^{8} tonnes from World Steel Association [40] and BorTec [41], and 1.13×10^{6} tonnes stated by Jaganmohan [42] respectively. The weightages are obtained through the AHP method through hierarchical pairwise comparison by judgement that considers the goal (best cathode), criteria (nickel recovery, electrical resistivity, current efficiency and material availability) and alternatives (AISI 304 stainless steel, graphite and nickel) networks and tally with the sensitivity analysis, obtainina g weightages' inconsistency of 1.97%. The analysis of the best cathode selection by the TOPSIS method considers the weightages obtained from the AHP method and the data obtained for all cathodes according to the factors, where a normalized matrix was formed using the positive and negative factors to calculate the relative closeness degree of alternatives towards the ideal solution that determines the ranking of the cathode materials. The factors are taken to be positive aspects, except resistivity, in the TOPSIS analysis methods.

Nickel recovery has the highest weightage (0.66776) in this analysis method, followed by current efficiency (0.15794), electrical resistivity (0.10665), and material availability (0.06764). This is because nickel recovery is the most important factor in obtaining maximum yield of nickel extraction out of the sludge for better waste management and utilization commercially, followed by current efficiency that measures energy utilization on the electrowinning process, which indirectly influences costs as well. Electrical resistivity is the third ranking factor because electrical resistivity is inversely proportional to electrical conductivity, so that more electrons can move within the cathode material to attract more Ni^{2+} by forming ad-atoms or "islands" that serves as an energetically favourable site (active site) for nucleation between Ni^{2+} and cathode's surface as nickel electrodeposition with the increase of growth of nucleus formed from the ad-atoms provided that the applied potential or current is sufficient [10]. Material availability is the least considered commercial factor because the chosen material used for cathode in the electrowinning setup is more focused on the extraction performance and production that outweighs this factor, especially in electronics field and other fields requiring high purity nickel to prioritize performance and safety in their products, to avoid failure leading to catastrophic consequences such as loss of consumer's trust, safety hazards, and worsened brand integrity and economy, which is much costlier than larger investments in better material for product performance. For instance, Apple's "Bendgate" issue in iPhone 6 and 6 Plus could be overcome by using a metal better than aluminium as the phone cover, which bends under pressure of being stored in a trouser pocket [43]. Based on the results generated from the AHP-TOPSIS analysis method in Table 3, the best commercial cathode material type in electrowinning is nickel metal in this case, with a score of 0.60, followed by graphite (0.49) and AISI 304 stainless steel (0.47). A larger investment is required for the high initial capital cost to save on the operating cost and other costs in the long run to obtain maximum yield of deposited nickel with the utmost purity, as nickel is the most expensive among the cathodes due to low material availability.

Table 3. Determination of the best cathode material type based on factors with their weighing factors using the AHP-TOPSIS method

Factor	Weightage	Types of Cathode Materials		
		Nickel	AISI 304 Stainless steel	Graphite
Ni^{2+} recovery (%)	0.66776	55.90	50.66	56.74
Current efficiency (%)	0.15794	24.35	6.09	39.57
Electrical resistivity (Ω·m)	0.10665	6.84×10^{-8}	7.20×10^{-7}	4.00×10^{-6}
Material availability (tons)	0.06764	2.69×10^{6}	6.14×10^{8}	1.13×10^{6}
Material performance index	1.00000	0.60	0.47	0.49

In terms of industrial application challenges, electrowinning using a nickel cathode has fewer complexities and is more feasible compared to other recovery methods such as adsorption, chemical precipitation, and ion exchange, for it has efficient recovery of Ni^{2+} with minimal reagent and energy utilization as well as high nickel selectivity [9]. This method, with simple setup and materials, is also easier to scale up to be utilized industrially with simpler process control and optimization, plus minimal maintenance and equipment wear, as it is a reliable and cost-effective stabilization process after treatment with direct electrodeposition onto the cathode, unlike other recovery methods. The final product of electrowinning is a high quality thickened nickel cathode by diameter, which can be readily utilized into the electroplating setup as the anode or other applications, being more sustainable, whereas other recovery methods are either difficult or cannot be reused such as nickel precipitation chemically that does not bind as a slab immediately and liquid nickel regeneration by removing from anionic polymer beads or adsorbents through uninstallation of the ion exchanger or adsorption column respectively that require solidification through electrowinning, chemical precipitation or other solidifying methods. This condition shows that electrowinning requires fewer steps, which saves more on labor, equipment, and other costs overall, resulting in cost implications and being more profitable compared to other recovery methods. Table 4 shows the details of technology adaptation or commercialization cost in the commercial world versus the approximation from this study.

For this technology adaptation or commercialization, cost comparison is only done for solvent extraction and electrowinning between the commercial world and, in this study, after scaling up as shown in Table 4, rather than the whole hydrometallurgy process, assuming other parts of the hydrometallurgy process require the same costs together with equipment, operating, and labor costs. Overall, initially, the capital cost is very high but less than the commercial one. In the long run, approximately after 5 years or more of payback period, the production of nickel through electrowinning is cheaper than the market price, and profit will start to come into the business. The net return and positive cumulative cash flow would be at a faster rate if more cells are built in the plant at large scale production. In fact, the cost of electrowinning to recover nickel is also cheaper and more beneficial than the cost of treatment and disposal of nickel sludge. In summary, electrowinning as a valorization method is worth being commercialized for utmost purity and yield of nickel, as it is economically feasible and sustainable in the long run, as it does not bring any byproduct waste and reduces the waste's hazard level towards the environment, plus saving the global nickel resources from extinction. However, the scale up production need to be done through pilot plant first, and adjust the electrowinning parameters of pH, electrical potential and contact time to be optimal if the optimized operating parameters in this study is not suitable as the mass transport, electrical properties, thermodynamics, chemical reactions, and other influencing aspects, with its conditions changed accordingly when upscaling to ensure maximum nickel recovery using nickel metal cathode. Thus, strategic and careful planning with proper approaches and risk management are required for successful commercialization. For future work, it is better to employ current-controlled methods [47], such as galvanostatic cyclic voltammetry, pulsed current and step current, rather than potentiostatic cyclic voltammetry used in this study. This is because current-controlled methods are more advanced and can yield better results, especially nickel recovery, compared to the traditional potentiostatic cyclic voltammetry, as the weight of deposited nickel is directly proportional to applied current according to Faraday's Law [48].

3.2. Cyclic Voltammetry

Theoretically, the electrooxidation shows that nickel becomes Ni^{2+} ion and releases 2 electrons in forward scan, followed by electroreduction, where Ni^{2+} ion accepts 2 electrons to form nickel in reverse scan. With all these reactions happening, peaks at the forward and reverse scan should appear on the cyclic voltammetry graph, but in this case, there are no peaks detected by the potentiostat software in the peak search analysis for all cathode material types, as shown in Figures 4 (a), (b), and (c). The curves are relatively smooth for all cathode material types, and the absence of anodic and cathodic peaks means that the redox reactions are irreversible, as stated by Salmani *et al.* [49], which is not possible practically. The absence of the peaks means that there is a thin film on the cathodes, as stated by Cursaru *et al.* [50], which is speculated to be the surface finish in the production of the cathodes. The situation also shows that the energy supplied by the applied voltage is not enough for the reactions to be achieved and shown in the

Table 4. Cost comparison of 1 cell for electrowinning commercialization to produce 200 kg of nickel per day

Category	Reference	Commercial (USD)	Study (USD)
Capital cost for solvent extraction	[44]	106,818.18	42,389.04
Capital cost for electrowinning	[44]	115,909.09	45,996.62
Cathode cost/kg	[45, 46]	1.77 (stainless steel)	16.75 (nickel)
Total cost	-	222,729.04	88,402.41
Total cost per kg of nickel	-	1,113.65	442.01

* Conversion rate of USD to RM on 26th June 2024 is USD 1 to RM 4.71.

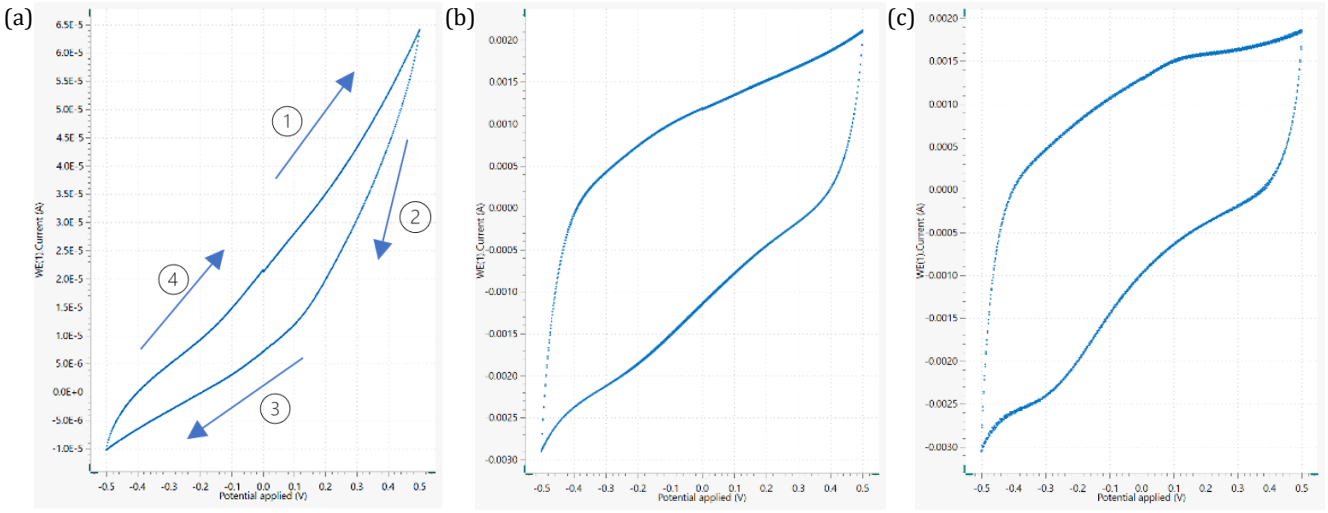

Figure 4. Cyclic Voltammetry curve of (a) graphite, 1. Oxidation Ni^{+} to Ni^{2+}, 2. Reduction of Ni^{2+} to Ni^{+}, 3. Reduction of Ni^{+} to Ni, 4. Oxidation of Ni to Ni^{+} (b) nickel metal and (c) AISI 304 stainless steel

graph, thus further study is required to overcome the film and to see the reactions better using larger range of applied voltage higher than 0.5 V and lower than −0.5 V. This condition is good as the only reaction that can occur in this electrochemical system is the nickel reduction, and no other undesirable reactions, such as evolutions or precipitation, present in the system, that makes the results of this study to be more accurate and precise. Further study on this section can be done by removing the surface finish to see more reactions in cyclic voltammetry through sandblasting and other methods, which could potentially give more insights. If the redox reactions are to be studied in this study, the cyclic voltammetry is required to be done at higher voltages than 0.6 V to know the reactions that are happening at the electrodes in the electrolyte, which involves the precipitation and evolutions, rather than having smooth peaks that cannot detect the redox reactions because it happens at a very low rate. The diffusion layer can be found through the diffusion coefficient with time, plus implementing Fick's second law (for planar electrodes) to do mass transport studies better in the future [27].

3.3. Optimization of the Electrowinning Process Condition

Table 5 shows the result of the electrowinning optimization process. From the result, the ideal electrowinning process setting is pH 5, 1 hour, and 0.5 V, resulting in a nickel recovery of 70.18% in run 6. Conversely, the worst process circumstances correspond to pH 5, 1 hour, and 0.6 V, resulting in a nickel recovery of 47.45%. These settings indicate that the electrical potential has the most substantial influence on nickel recovery, superseding pH and contact time as determining factors. The reason behind this situation is that the nickel recovery is inversely proportional to electrical potential but must match the electron energy required to reduce Ni^{2+} to Ni, vibrating most at the right electronic level (applied electrical potential) [6]. The stability of the results is demonstrated by coefficient of variation of 10.19%, derived from a standard deviation of 5.92, showing high stability and consistency within the data, and can be supported further with the mean absolute error and root mean square error of 3.42 and 4.08 that give a low 5.89% and 7.01% (< 10%) of the mean predicted results of 58.12 with mean squared error of 16.61. Nevertheless, the experimental ideal electrowinning parameters of pH 5, 1 hour, and 0.5 V, which resulted in a nickel recovery of 70.18%, may lack accuracy due to uncontrolled errors and phenomena that interfere with the precision and correctness of the results. Thus, by employing statistical analysis, the unfavorable circumstances are considered and eliminated to achieve the statistically optimized electrowinning conditions. This allows for the development of an ideal model for optimizing the study with the utmost accuracy and precision. Additionally, it provides a more profound understanding of the interdependence and influence of the factors on nickel recovery, which is the aim of the study.

With the data obtained from the experiment based on Table 5, in Table 6, the model is the best fit as a linear model equation with a p-value of 0.0262 (< 0.05), which means the study is significant, including the intercept, pH, contact time, and electrical voltage. The model F-value is 4.28, which shows that the study is significant that at least one factor is significant, where only 2.62% chance that the large F-value can occur due to noise, which means the ANOVA analysis of this study rejects the null hypothesis, saying this study is not significant or does not have an impact. The lack of fit F-value is 0.9882, which means that the lack of fit is not significant relative to the pure error, which is good that defines the model is adequate and fitting with 54.95% chance that it occurs due to noise, with adequate precision of the data is 6.501 (> 4), making the study desirable at ratio of signal to noise used to navigate the design space. Moreover, it shows that pH and contact time are not significant (p-value > 0.05) with p-values of 0.3497 and 0.2373, respectively, whereas electrical potential is significant (p-value = 0.0067) in this study. This means that only electrical potential can hugely impact the study more than pH and contact time, proven from Figure 5(a) where R^2, adjusted R^2 and predicted R^2 of 0.4971, 0.3810 and 0.1071 are quite low, where the

Table 5. Optimized conditions for the electrowinning process result

Run	Parameters			Nickel Recovery Result	
	pH	Contact Time (hour)	Applied Potential (V)	Actual Recovery (%)	Predicted Recovery (%)
1	4	3	0.55	48.31	54.48
2	6	2	0.60	54.89	54.41
3	5	2	0.55	58.33	58.12
4	6	3	0.55	54.49	57.68
5	6	1	0.55	62.70	61.76
6	5	1	0.50	70.18	65.47
7	4	2	0.60	57.14	51.22
8	5	2	0.55	64.16	58.12
9	4	2	0.50	60.84	61.83
10	5	3	0.60	54.66	50.77
11	5	3	0.50	62.55	61.39
12	5	2	0.55	55.07	58.12
13	4	1	0.55	56.02	58.56
14	6	2	0.50	63.02	65.03
15	5	1	0.60	47.45	54.86
16	5	2	0.55	54.38	58.12
17	5	2	0.55	63.89	58.12

Table 6. Optimized conditions for the electrowinning process result

Source	Sum of Squares	df	Mean Square	F-value	p-value	Significance
Model	279.11	3	93.04	4.28	0.0262	Significant
A-pH	20.44	1	20.44	0.9410	0.3497	
B-Time	33.33	1	33.33	1.53	0.2373	
C-Electrical Potential	225.34	1	225.34	10.37	0.0067	
Residual	282.38	13	21.72	-	-	
Lack of Fit	194.78	9	21.64	0.9882	0.5495	Not significant
Pure Error	87.60	4	21.90	-	-	
Cor Total	561.49	16	-	-	-	

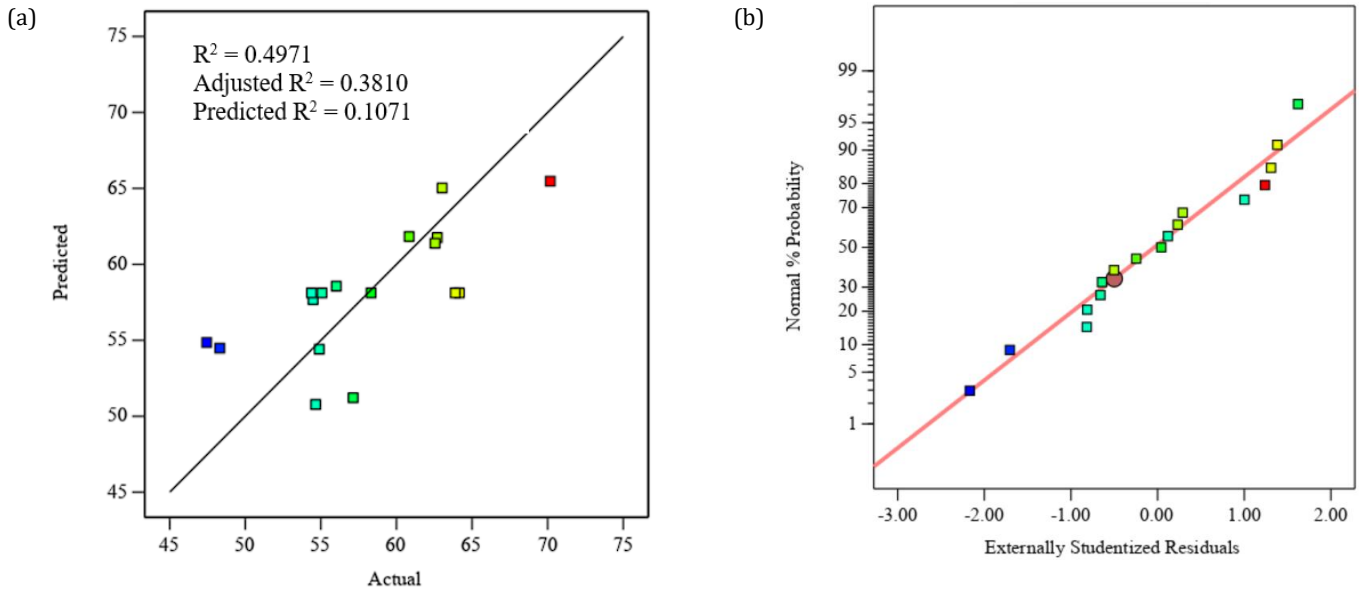

Figure 5. (a) Predicted vs actual data graph, and (b) normal plot on nickel recovery of this study

relationship between factors and nickel recovery is relatively weak and harder to predict experimental responses using this model due to the large variation of data determined by the model that creates outliers and deviates all the R^2, plus only 1 out of 3 factors strongly influence nickel recovery, where any data out of the predicted range can heavily impact the correlation that is determined from a very small number of runs. Additionally, data in optimization contains very good and bad results for varying sets of parameters, giving huge variations that are not easily averaged or obtained within a small range, like the predicted values by the system. Thus, it is safe to say that the model can be used to predict well for electrical potential and use pH and contact time as guide for they are still vital and contribute to the study, to obtain the highest yield of nickel recovery due to their significance in the model that gives influence towards the response.

For Figure 5 (b), the experimental results of nickel recovery are quite closely aligned to the normal line that shows quite homogeneous variances in the normally distributed residuals that are not correlated with each other as stated by Tee *et al.* [51], proving the model fits the data and interpretable with random errors, rather than systematic, in the range of pH, contact time and electrical voltage as factors in this study for the chosen design model of Box-Behnken. All the factors are statistically independent and are not correlated because they are orthogonal with variation inflation factors of 1 according to the ANOVA analysis. This model possibly captures the main relationships in the data, where blue color indicates the lowest nickel recovery (47.4467%) and increases to green, yellow, orange, and red as the highest nickel recovery (70.18%).

For optimization in this study, the constraint assumptions applied are having all factors of pH, contact time and electrical voltage to be in their own range as the lower and upper limit respectively (pH 4 to pH 6; 1 hour to 3 hours; 0.5 V to 0.6 V) with importance values of 3, 4 and 3, respectively, whereas the response of nickel recovery is set to maximum as the goal of this study with 47.45% and 70.18% as the lower and upper limit respectively with the highest importance value of 5. The lower weight and upper weight of each factor are 1. Therefore, with all the experimental data, chosen ANOVA model, constraints, and the design type of response surface methodology (Box-Behnken Design), the optimal electrowinning conditions are pH 6, 1 hour, and 0.5 V with 70.18% nickel recovery. The model equation of the study by ANOVA is shown in Equation (5), where A is the pH, B is the contact time (hours), and C is the electrical potential (V).

$$\text{Nickel recovery (\%)} = 58.12 + 1.60\,\text{A} - 2.04\,\text{B} - 5.31\,\text{C} \quad (5)$$

Figure 6 demonstrates the correlation between the variables and nickel recovery. Figure 6 (a) displays a contour graph indicating that the red region at pH 6 and 1 hour yields the highest nickel recovery, around the point of 66.54% at a desirability of 0.838539 in this work at 0.5 V. The recovery then gradually decreases from red to orange, yellow, and finally to the green region, depicting the lowest recovery around the point of 61.2862% at a desirability of 0.613253 for 0.5 V. In Figure 6 (b), the contour graph indicates that the green region at pH 6 and 1 hour yields the highest nickel recovery, around the point of 55.5929% at a desirability of 0.361306 in this work at 0.6 V. The recovery then gradually decreases from green to cyan, concluding in the blue region with the lowest recovery around the point of 50.239% at a desirability of 0.11163 for 0.6 V.

Comparing Figure 6 (a) and (b), the nickel recovery at 0.5 V ranges from average to maximum (green to red region), while at 0.6 V it ranges from minimum to average (blue to green region). This implies that at 0.55 V, the nickel recovery is average throughout the entire region, visible only as green without any contour. Figure 6 (c) and (d) both exhibit similar patterns in terms of contour colors and regions when viewed from a three-dimensional perspective. Additionally, the height of the plane from the ground suggests that the nickel recovery in Figure 6 (c) at 0.5 V is greater than that in Figure 6 (d) at 0.6 V. Both 3D graphs indicate that the plane is flat without curvature. This suggests that the model is of a linear type with an inclination, where the nickel recovery at the y-axis increases from pH 4 to pH 6, while at the z-axis and x-axis, it increases from 3 hours to 1 hour based on the contour and inclination height of the developed model.

As for pH, the optimal Ni^{2+} recovery is achieved at pH 6. The reason for this is that the hydrogen and oxygen evolutions at the cathode and anode are less intensive at pH 6 compared to pH 4 and pH 5. Both reactions impede the deposition of nickel onto the cathode, shifting the focus of the energy to undesirable reactions. This condition signifies that a more alkaline pH is suitable for the experiment to achieve the highest nickel recovery. This is true in the study by Hou *et al.* [52] and in the practical experiment, as it does not induce hydrogen evolution in alkaline situations due to a lack of H^+. The hydrogen evolution reaction rendered the electrodeposited nickel less firmly bonded to the cathode due to the attraction of Ni^{2+} through opposite ionic charges, giving a less sturdy form of deposited structure and a worsened surface finish on the cathode. Moreover, Ni^{2+} must compete with H^+ for the provision of electrons to be reacted at the cathode, which further diminishes the recovery of Ni^{2+}, resulting in somewhat lower nickel recovery at pH 4. Yet, there is a possibility of ion precipitation that drags along Ni^{2+} at pH 6, occurring in an alkaline environment, reducing the deposition yield. This is because the acidity of H^+ ions is rapidly absorbed at the cathode, causing a gradual increase in pH, and even more rapid when the initial pH of the electrolyte is closer to neutral, namely pH 7, due to a lack of H^+. Despite the production of H^+ at the anode by the degradation of water molecules, the rate of hydrogen evolution is far higher, where water is mostly utilized for the ionization of $NiSO_4$, resulting in the formation of Ni^{2+} and SO_4^{2-}. Thus, the pH of the electrolyte needs to be accurate and strictly controlled to pH 6, but never exceed.

Considering the aspect of interaction time, 1 hour is the most adequate duration, as opposed to 2 hours and 3 hours.

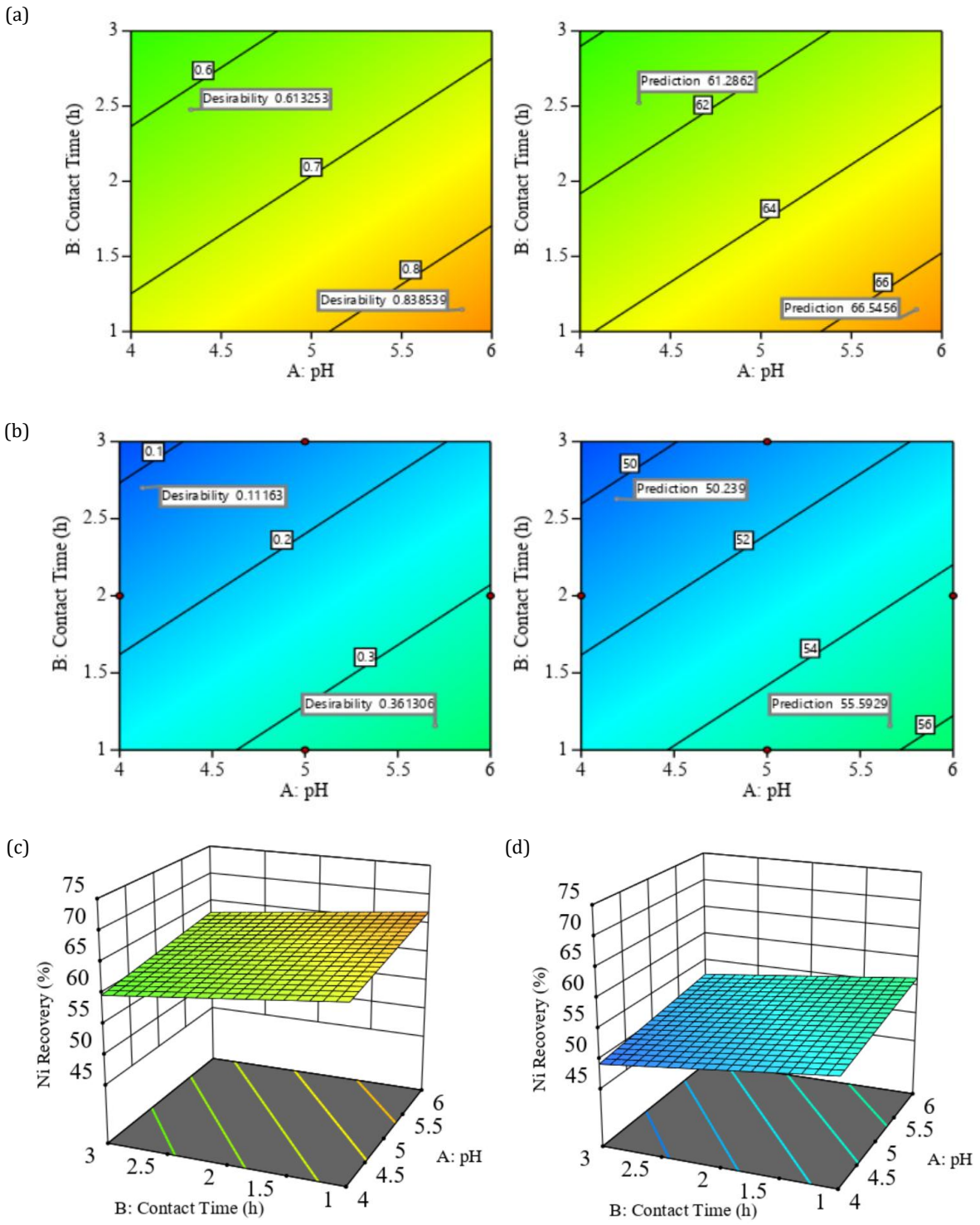

Figure 6. Contour graphs of desirability with nickel recovery at (a) 0.5 V and (b) 0.6 V, and 3D graphs of nickel recovery at (c) 0.5 V and (d) 0.6 V

Since this electrochemical system is a multistep electron transfer system that transfers one electron at a time, more time is needed to transfer two electrons for complete reaction, it is advisable to extend the contact time as much as possible to allow Ni^{2+} bond at the active sites (micropores) to deposit as solid metal on the cathode, as stated by Sudibyo *et al.* [19]. Nevertheless, a duration of 1 hour is adequate due to the very small surface area of the cathode and the limited supply of Ni^{2+} in the electrolyte, which amounts to 10,300 mg/L and will not be added on (finite supply) as the nickel deposition is already completed by 1 hour from observation during the experiment. As the experimental time required is less for a better yield, it is suitable for a pH 6 electrolyte as it will reduce the possibility of precipitation if the phenomena were to occur during the electrowinning process [19].

When considering electrical potential, a value of 0.5 V is optimal for maximum recovery of Ni^{2+}, surpassing the values of 0.55 V and 0.6 V. Assuming that a higher electrical potential will supply more energy to Ni^{2+} for migration, it is self-supporting on account of the absence of supporting ions as described by Compton *et al.* [27]. Additionally, it provides enough energy to overcome the ohmic resistance of the electrolyte, the electromotive force of chemical reaction (ion diffusion and charge transfer), and the electromotive force caused by anode polarization [53]. Low voltage is better for the system based on the analysis because too much energy supplied can induce hydrogen evolution and precipitation, which hinders nickel deposition onto the cathode, plus the product gets oxidized and forms nickel oxide as black flakes due to anodic oxygen evolution. A higher applied potential may also risk the safety of the experiment, where sparks and fire can occur due to the small area of the cathode and its electrical conductivity. In this case, the reduced electrical potential of 0.5 V is sufficient to surpass all the obstacles and amplify the electric field surrounding the cathode by utilizing the electrical conductivity of nickel to align Ni^{2+} towards the cathode through a stronger electrochemical gradient as the driving force, rather than allowing them to freely rotate in the electrolyte. Once the potential difference between the working electrode (cathode) and the electron transfer plane reaches a sufficient magnitude, Ni^{2+} can be promptly reduced at the surface of the cathode [27].

Therefore, after analyzing the data using ANOVA, the findings showed that this model developed through Box-Behnken Design is significant and well-fitted, but also found that only electrical potential significantly affects the nickel recovery greatly, whereas pH and contact time act as complements to electrical potential due to the lesser significance towards the response of this study. The optimal parameters in the study would be pH 6, 1 hour, and 0.5 V with 70.18% nickel recovery. Although pH and contact time are not significant, they may relate to the electrowinning process as the events that happen when deviated from these optimal conditions, such as precipitation, evolution of gases, and many more, would really happen as observed during the experiment.

3.4. Surface Morphology

Figure 7 (a) to (f) shows the image of the cathode for Runs 2, 14, 3, 10, 4 and 16, respectively, while Figure 8 (a) to (f) shows the image of surface morphology of the same run as the image of the cathode. From Figure 8 (a), the deposited nickel layer on the cathode has a roughly equiaxed grain structure with a nearly random grain orientation distribution, as stated by Dawson [54], where the small grains are precipitates of sodium (18.1%) and nickel (81.9%) according to the EDX analysis. In comparison with Figure 7 (a), the visually deposited nickel layer has a rough texture topographically and scattered with small round grains of precipitate crystals crystallographically, morphogically and compositionally, which matches the SEM and EDX analysis in Figure 8 (a). The cathode of Run 2 in Figure 7 (a) and Figure 8 (a) was run at pH 6, 2 hours and 0.6 V, which means precipitation and evolutions occurred since the energy supplied at 0.6 V is too much that induce the reactions, plus the contact time is exceeded the optimized time of 1 hour, which gives more opportunity for the reactions to occur, that hindered the nickel recovery, only resulting to a low value of 54.89%.

According to Figure 7 (b), the deposited nickel layer on the cathode has a bright and dark surface on the left and right, respectively. The bright surface is nickel (100%), and the dark surface's composition contains 56.6% sodium and 43.4% nickel, as shown in Figure 8 (b). The topographic perspective of the bright surface shows smooth multicrystalline layers of nickel deposited stated by Satyanarayanaraju & Krishnamurthy [55] and Peshcherova *et al.* [32], whereas the dark surface is a big spot or flake of nickel and sodium deposited, which is similar to the visual situation of the cathode in Figure 7 (b) with smooth and segregated texture topographically, and large, heavy flaky nickel layers deposited on the surface morphologically, where the flakes are stacked crystallographically, and can be taken off easily due to very heavy deposit of silvery nickel for it reaches high nickel recovery of 63.02% when this cathode run at pH 6, 2 hours and 0.5 V. The voltage has given the correct amount of energy and has a pH 6 as the conducive environment, but 2 hours is too long; nickel is heavily deposited onto the cathode to the extent that it can be peeled off on its own.

For Figure 8 (c) and (d), the deposited nickel on the cathodes has discontinuous multicrystalline layers with small grains and its boundaries of nickel (100%) stated by Leiva-García *et al.* [31] and Peshcherova *et al.* [32], where the grains are more obvious on the cathode in Figure 7 (c) than that in Figure 7 (d). This characterization is proportional to the nickel recovery, proving that the nickel recovery of the cathode in Figure 7 (c) is 58.33%, which is higher than that of the cathode in Figure 7 (d) with 54.66% nickel recovery. The cathodes in Figure 7 (c) and (d) show considerable or acceptable deposited surface visually, where the cathode in Figure 7 (c) runs at pH 5, 2 hours and 0.55 V, and the cathode in Figure 7 (d) runs at pH 5, 3 hours and 0.6 V, respectively. The reason of the higher nickel recovery on cathode in Figure 7 (c) than cathode in Figure 7 (d) is because the voltage applied is lower (0.55 V < 0.6 V),

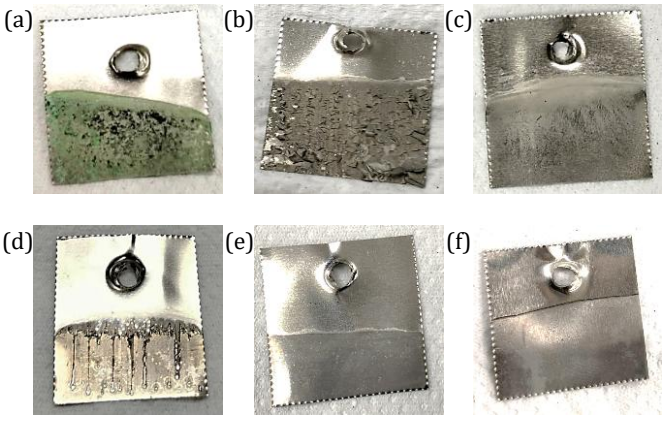

Figure 7. Image of the ideal commercial cathode material type for (a) Run 2, (b) Run 14, (c) Run 3, (d) Run 10, (e) Run 4, (f) Run 16

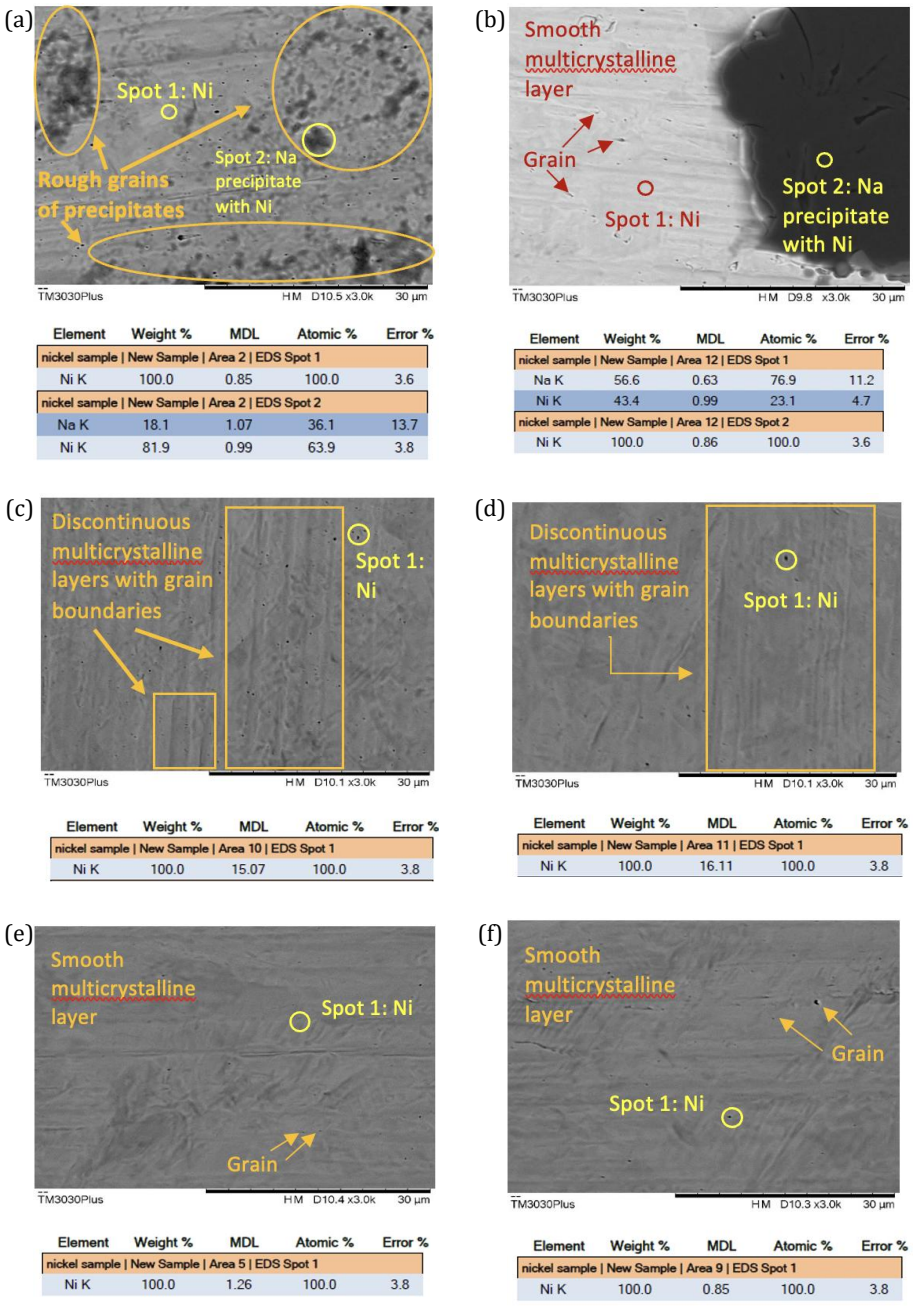

Figure 8. SEM and EDX of the ideal commercial cathode material type for (a) Run 2, (b) Run 14, (c) Run 3, (d) Run 10, (e) Run 4, (f) Run 16

giving a more suitable energy to the electrowinning process, which do not have black nickel oxide with circles due to hydrogen evolution as shown in Figure 7 (d), and the contact time is lower as well (2 hours < 3 hours), reducing the undesirable situations to potentially occur plus giving uneven surfaces.

For Figures 8 (e) and (f), the deposited nickel on the cathodes is a smooth multicrystalline surface with very few small grains, as stated by Satyanarayanaraju & Krishnamurthy [55] and Peshcherova *et al.* [32], with a composition of nickel (100%). The characterization matches the visual outcome of the cathodes in Figures 7 (e) and (f), which are smooth and compact. However, the cathode in Figure 7 (f) is a little grainier than the cathode in Figure 8 (e), which is exactly shown in the SEM images in Figure 8 (e) and (f). Moreover, the nickel recovery for both cathodes in Figures 7 (e) and (f) is quite low, with 54.49% and 54.38% respectively. This situation may be because the cathode in Figure 8 (e) runs at pH 6, 3 hours, and 0.55 V, and the cathode in Figure 7 (f) runs at pH 5, 2 hours, and 0.55 V, where the optimized parameters are not executed in either run.

Overall, the cathodes in Figure 8 (a) and (b) do not have a good characterization of the nickel deposition; the cathodes in Figure 8 (c) and (d) have an average characterization, whereas the cathodes in Figure 8 (e) and (f) have very good characterization. The characterization analysis on the cathodes in Figure 8 (a) to (f) reflects the quality of the visually deposited nickel product on the cathodes in Figure 7 (a) to (f). There is a good protective film shown on the

cathodes in Figure 8 (c), (d), (e) and (f), stated by Giwa *et al.* [34], whereas precipitation and hydrogen evolution would affect the product's characterization in Figure 8 (a) and (b). However, good characterization may not necessarily mean that the nickel recovery is good as well.

3.5. Kinetic Study

3.5.1. Nernst Equations

The Nernst equation is based on cyclic voltammetry and is used to determine the formal potential of an electrochemical system, with the assumption of kinetics of electron transfer are fast relative to the rate of mass transport [27]. In reference to the Nernst equation for nickel reduction derived by Md Ali [10], the Nernst equation in this study is derived from the measured potential in this electrochemical system operating at conditions of pH 6, 0.5 V and 2 hours using nickel metal in treated nickel sludge as electrolyte, where the result of negative electrical potential is more favourable as the nickel ions are mostly reduced and deposited onto the surface of the cathode in the negative electrical potential at a normal environment. At standard atmospheric pressure (1 atm) and temperature (298 K), where universal gas constant, R, is 8.314 $J \cdot K^{-1} \cdot mol^{-1}$, valency, n, is 1 for one electron transfer at a time and Faraday's constant, F, is 96485 $C \cdot mol^{-1}$ in Equation (1) with the initial condition of the electrochemical system is 99.80% Ni^{2+} and 0.20% supporting ions, the final Nernst equation derived for this study is shown in Equation (6).

$$E_{Ni^{2+}/Ni}(\text{SCE 3.5M})/V = -0.4776 + 0.0296 \log[Ni^{2+}] \quad (6)$$

It is found that the formal potential of this electrochemical system is –0.4776 V (SCE 3.5 M), which is less negative than that in the study of Md Ali [10] (–0.4905 V (SCE 3.5M)). This is because the content of Ni^{2+} in this study is much more than that in the study by Md Ali [10] (99.80% > 0.15%), where this current study only focuses on one reaction compared to the previous study that have many other reactions involved and competing against each other to be reacted, although the concentrations of Ni^{2+} is similar in both studies. Hence, lesser energy is required for Ni^{2+} to deposit on the surface of the cathode as they can be done more spontaneously at a faster rate without competing against other reactions, plus being able to be transported through the chemical gradient, rather than the diffusion mechanism, as the driving force in the current study than that in the previous study. Thus, the formal potential of nickel reduction using a nickel cathode in treated nickel sludge as electrolyte under normal conditions is –0.4776 V (SCE 3.5 M).

3.5.2. Butler Volmer Equations

The Butler-Volmer equation can be derived from the linear sweep voltammetry, where only this voltammetry includes current density, which is a component of the equation. This single equation explains the kinetics of the redox reactions, which is more comprehensive and general compared to the Tafel equation. According to Figure 9 (a), the gradient of the graph is 0.8865, and the anodic alpha value is obtained as 0.05245. Thus, the cathodic alpha value is 0.94755, as the sum of cathodic and anodic alpha values is equal to 1. From the extrapolation of the graph in Figure 9 (b), the extrapolated value obtained on the axis of log of equilibrium exchange current density is –4.74, thus the equilibrium exchange current density of the electrochemical system, i_o, is 1.8197×10^{-5} A/cm^2. The current density is 0.00025 A/cm^2, where the applied current in the system is 0.001 A and the area of the cathode is 4 cm^2. With all these values substituted into Equation (7), which is Butler Volmer equation with the approximation of high overpotential, where the cathodic part of the original equation becomes negligible, in this system at 0.5 V (SCE 3.5 M) as the measured potential, the electrical potential of equation or the formal potential is –0.7836 V (SCE 3.5 M), with 1.2836 V (SCE 3.5 M) as the overpotential of the system. The final Butler-Volmer equation in terms of voltage measured with a saturated calomel electrode (3.5 M) is shown in Equation (8).

$$\eta = \frac{2.303\,RT}{\alpha_a F} \log \frac{|i|}{i_o} \quad (7)$$

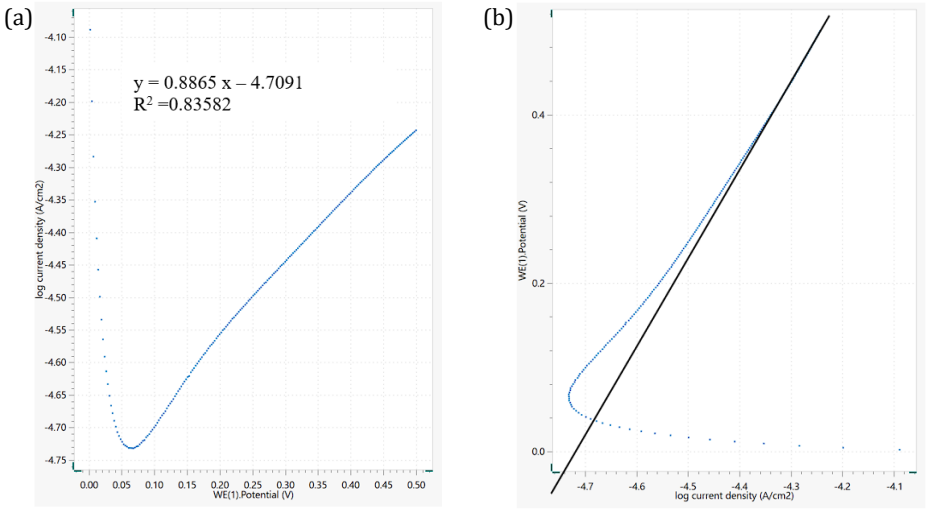

Figure 9. (a) Graph of log current density vs potential, and (b) graph of potential vs current density

$$i = i_o \left[\exp\left(\frac{11605.12 \propto_a (E + 1.2836)}{T} \right) - \exp\left(\frac{-11605.12 \propto_c (E + 1.2836)}{T} \right) \right] \quad (8)$$

From this result, the formal potential of this system in the Butler-Volmer equation is far more negative than that in the Nernst equation (−1.2836 < −0.4776 V). This may mean that −1.2836 V (SCE 3.5 M) is the minimum electrical potential of this system, and 1.2836 V (SCE 3.5 M) is the maximum electrical potential, so this electrical potential range is the widest range for this electrochemical system. However, the evolutions, precipitation and other undesirable reactions may occur together with the redox reactions, thus precautions and errors must be taken seriously. To prove this statement, further studies are required.

3.5.3. Tafel Equation

From the values found in the previous section (Butler Volmer Equation section) that are relevant to the Tafel equation in Equation (3) based on Figure 9 (a) and (b), the electrical potential of the system or the formal potential is 0.5711 V (SCE 3.5 M), with −0.0711 V (SCE 3.5 M) as the overpotential of the system. The final Tafel equation of this electrochemical system in terms of voltage measured with a saturated calomel electrode (3.5 M) is shown in Equation (9).

$$E = 0.5711 - (1.9845 \times 10^{-4}) \frac{T}{\alpha_c} \log \frac{|i|}{i_o} \quad (9)$$

The formal potential obtained from the Tafel equation is quite close to that of the Nernst equation. The additional value in the formal potential derived from the Tafel equation might be due to the resistances that are present in the electrochemical system, which are required to be overcome, such as the ohmic resistance and so on, in order to enable the redox reactions to occur. Thus, 0.5711 V (SCE 3.5 M) is the least maximum electrical potential and −0.5711 V (SCE 3.5 M) is the least minimum electrical potential of this system, which means for reactions to occur in this electrochemical system, the range of electrical potential applied must be at least from −0.5711 V (SCE 3.5 M) to 0.5711 V and cannot be less than these values. This does not mean that the applied potential of 0.5 V is invalid, because the value of 0.5 V is obtained through the Nernst equation by previous studies, where the Nernst equation is the most general equation that is valid for all concentrations of electrolyte.

3.5.4. Anson Equation

The chronoamperometry is done to allow Ni^{2+} contact with the active sites and deposit as nickel for 2 hours (for run 14), while supplying the energy through the applied potential of 0.5 V and −0.5 V by the potentiostat in a pH 6 electrolyte. Both positive and negative electric potentials are important during chronoamperometry, as nickel deposition can occur with these energies, as shown in Figure 10 (a) and (b), plus the positive voltage is to ensure that ions other than Ni^{2+} are precipitated and not deposited onto the cathode as impurities.

The Anson equation is based on chronoamperometry and is used to study the relation between the charge used for the reactions that is supplied through the current and the time in the electrochemical system. There are a few exceptions to the Anson equation in Equation (2) due to the nickel cathode being macro-sized (2 cm by 2 cm), which is bigger than the nanoscale. For macroelectrodes, the electrical double layer is negligible with respect to the depletion layer and charge balance stated by Compton *et al.* [27], which means Q_{dl} is zero, due to the electric field being null at the edge of the double layer to the distance for electron transfer (the diffusion region). From Figure 11 (a) and (c), the charge increases exponentially with a few instances of constant gradients when 0.5 V is applied to the electrochemical system. This situation can mean that the electrochemical system is trying to increase the current to further increase the charge input, which indirectly reduces the voltage, where charge is inversely proportional to voltage, so that Ni^{2+} is highly charged to be deposited onto the cathode surface through ion attraction in the electrical field around the cathode.

This reasoning applies the same to Figure 11 (b) and (d), but the charge increases gradually with longer constant gradients for the applied potential is −0.5 V, which is easier for Ni^{2+} to deposit onto the cathode surface at negative potential and does not need to extract so much energy from the potentiostat in short instances when it can overcome the resistances easier than the situation shown in Figure 11 (a) and (c). As the time increases, the deposition of Ni^{2+} onto the cathode's surface becomes harder, thus the charge increases more until the 7000th second mark, where the surface of the cathode is totally saturated and require much more energy for more Ni^{2+} to be deposited on very few free active sites or forcefully deposit at any point of the cathode, if stacking on the deposited nickel layer is necessary.

From Figure 11 (c), the slope is 0.83164, which is equivalent to the term of $2nFAC\ (D)^{0.5}/\pi^{0.5}$, where valency, n is 2, A is 4 cm^2, F (Faraday's constant) is 96485 $C \cdot mol^{-1}$, bulk concentration of Ni^{2+}, C is 1.75498×10^{-4} mol/cm^3, and π as 3.142 and Q_{ads} is equal to −18.835 based on Equation (2). The diffusion coefficient of Ni^{2+}, D at 0.5 V, is found to be 2.9602×10^{-5} cm^2/s from calculation. The final equation of the Anson equation at 0.5 V (SCE 3.5 M) is derived and shown in Equation (10).

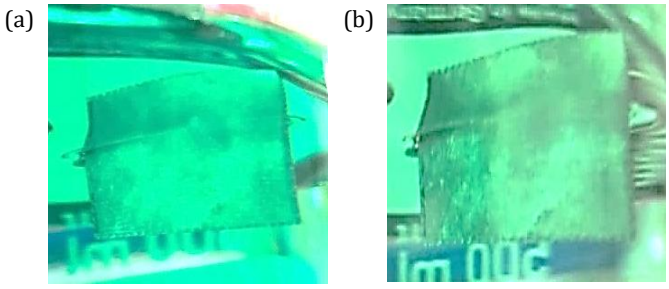

Figure 10. Nickel deposition onto the surface of the cathode at (a) positive voltage and (b) negative voltage

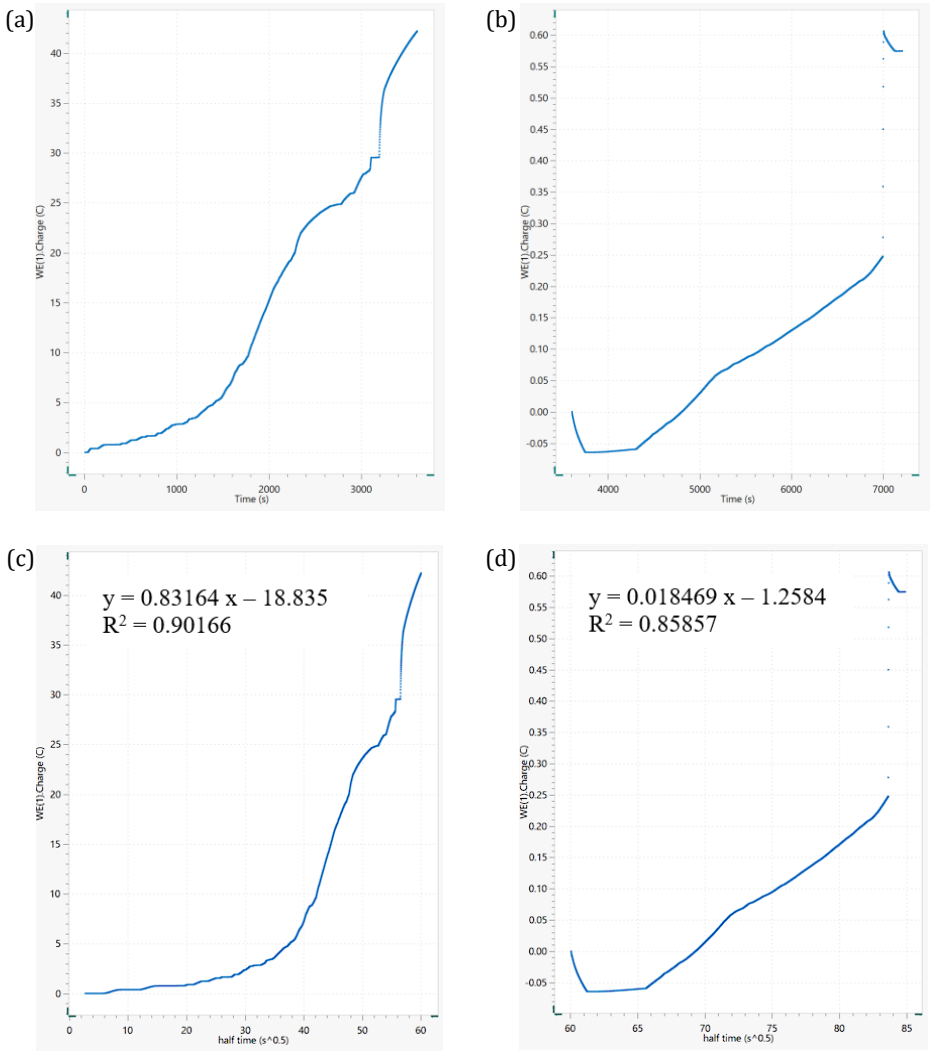

Figure 11. Graphs of charge vs time at (a) 0.5 V and (b) –0.5V, and graphs of charge vs square root of time at (c) 0.5 V and (d) –0.5 V

$$Q = 1184.69AC\ (t)^{0.5} - 18.835 \quad (10)$$

From Figure 11 (d), the slope is 0.018469, which is equivalent to the term of $2nFAC\ (D)^{0.5}/\pi^{0.5}$, where all constants except D are the same as mentioned previously and Q_{ads} is equal to –1.2584 based on Equation (2). The diffusion coefficient of Ni^{2+}, D at –0.5 V, is found to be 1.4599×10^{-8} cm^2/s from calculation. The final equation of the Anson equation at –0.5 V (SCE 3.5 M) is derived and shown in Equation (11).

$$Q = 26.31AC\ (t)^{0.5} - 1.2584 \quad (11)$$

From the derivations of Equations (10) and (11), the coefficients of $AC\ (t)^{0.5}$ in Equation (10) is much bigger than that in Equation (11) (1184.69 > 26.31) due to larger energy needed through charge supply by Ni^{2+} in the positive voltage environment at 0.5 V (SCE 3.5 M) to overcome the resistances of the electrolyte and the resistive electric field around the cathode to deposit Ni^{2+} onto the cathode's surface, thus the diffusion coefficient of Ni^{2+} in the positive voltage environment is larger because it need to move at a faster rate to capture electrons that have undergo tunnelling from the cathode while overcoming large resistances compared to that of Ni^{2+} in negative voltage environment at –0.5 V (SCE 3.5 M), having less resistive electric field around the cathode that Ni^{2+} does not require so much energy to deposit.

Furthermore, due to more resistances in the positive voltage environment at 0.5 V (SCE 3.5 M), the adsorption charge of Ni^{2+} is lower (–18.835 < –1.2584) for it is more difficult to deposit onto the cathode's surface in such environment to have a high efficiency of electron transfer between the cathode and Ni^{2+} compared to that of Ni^{2+} in negative voltage environment at –0.5 V (SCE 3.5 M). Thus, for maximum nickel recovery, more charge is required for Ni^{2+} to travel and obtain the electrons to transform into Ni on the cathode's surface, plus having more energy to conquer the resistances present in every perspective of the electrochemical system. In addition, the application of negative electrical potentials will give a more conducive environment for Ni^{2+} to form Ni on the cathode's surface.

Moreover, during the experimental run for the contact time parameter through chronoamperometry, the electrical potential of the electrochemical system is also measured to see any changes that occur throughout the whole experiment. From Figure 12 (a), the applied electrical potential remained constant most of the time at 0.5 V, but

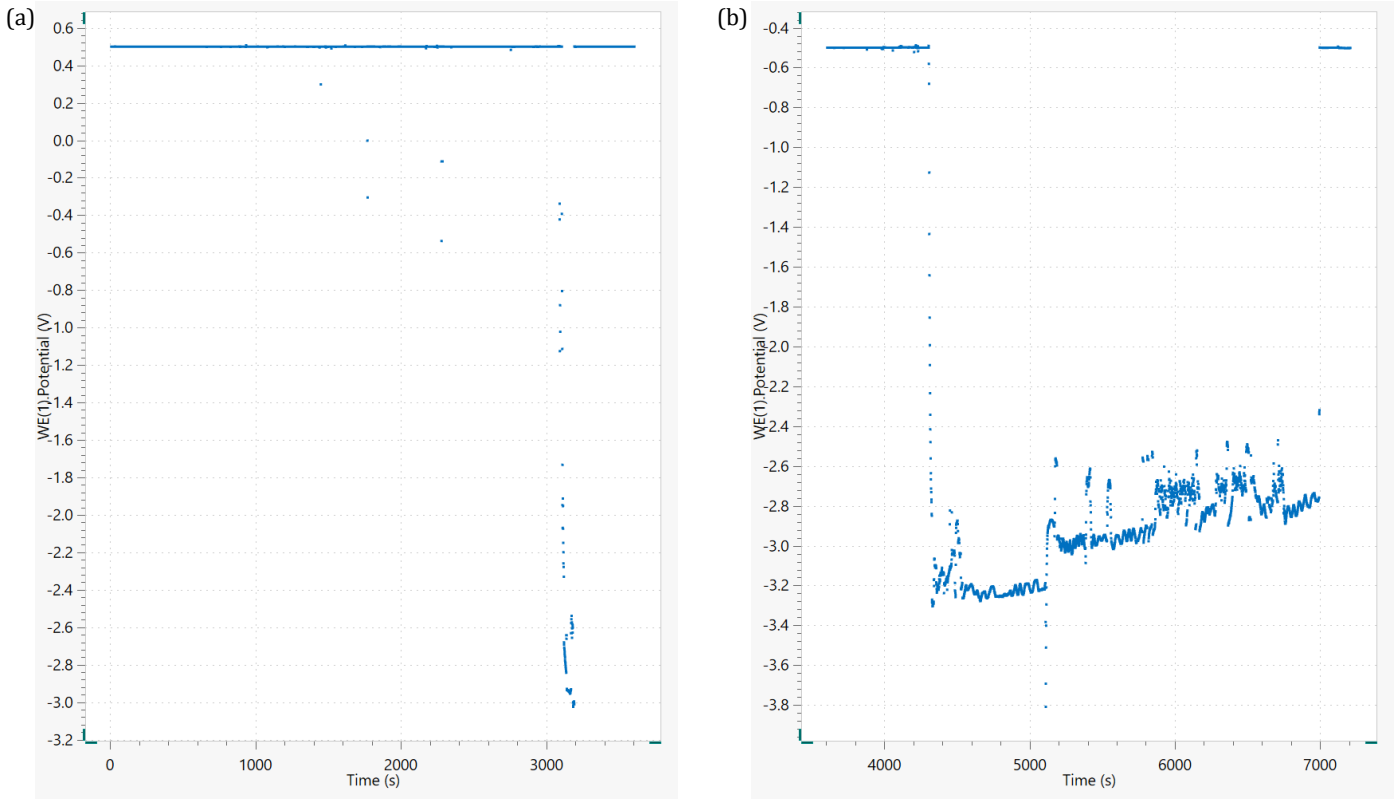

Figure 12. Graph of potential vs time at (a) 0.5 V and (b) –0.5 V

there are some drops in electrical potential for small instances seen that range from 0.1 to –3.0 V. For Figure 12 (b), the applied electrical potential of –0.5 V remained constant for 700 s, and then dropped to a range of –2.4 V to –3.4 V for 2688 s (out of 3600 s), and even further to –3.8 V for a small instance at 5,111th second mark. This has proven that the maximum electrical potential of the system can be up to –1.2836 V (SCE 3.5M) from the derivation of the Butler Volmer equation previously.

The additional negativity of the electrical potential may be because of the resistances that are required to overcome to deposit Ni^{2+} on active sites of the cathode, plus the number of active sites decreases with more and more nickel deposition, thus more energy (more negative electrical potential) is required to deposit more Ni^{2+} until the cathode is saturated with Ni. This occurrence of this situation is also because the potential changes at the cathode surface interface from the cathode's potential to the electrolyte's potential over a much larger distance, which is beyond the electron tunnelling distance (region for mass transport of Ni^{2+} between cathode and electrolyte for deposition) [27].

To explain the reason behind the huge drop in electrical potential beyond the applied voltage to the electrochemical system, Ni^{2+} undergo electrolysis near the cathode and will be influenced by the charge on the cathode through attraction or repulsion of charge while experiencing an electric field around the cathode, which makes electron tunnelling easier to achieve for deposition onto the cathode's surface, instead of diffusion due to the environment of lack of supporting ions (ions other than Ni^{2+}) [27]. When Ni^{2+}, the electroactive species in the electrochemical system, is highly charged by the electric field, Ni^{2+} contributes to the compensation of the electrical charge acting on itself as the supporting electrolyte, as stated by Compton *et al.* [27], which means Ni^{2+} is the supporting ion itself. This self-support capability of Ni^{2+} is also responsible for the reduction of the electrolyte's resistivity to achieve maximum nickel deposition onto the cathode. Thus, at short times, response is mainly controlled by ohmic drop effects, which is the loss in driving force of electron transfer to Ni^{2+}, and as the time increases, the charge excess is gradually dispersed and potential drop decreases to a certain period where the potential difference between the cathode and the plane of electron transfer region of 10 to 20 Å in the electrolyte is large enough for immediate reduction of Ni^{2+} at cathode's surface with full thermodynamic force to drive the reaction across the region as the electron tunnelling is efficient over a short distance of a few Å due to electromigration of flux of Ni^{2+} towards the cathode's surface [27].

In addition, during the experiment, there are no other undesirable reactions, such as evolutions and precipitation, occurred in the electrochemical system even though the voltage drops to very negative electrical potentials, which means that the voltage drop is induced by the system itself voluntarily. Therefore, the electrochemical system is induced by a charge that causes the voltage to drop for the deposition of Ni onto the cathode's surface. Thus, for maximum nickel recovery, more charge is required for Ni^{2+} to travel and obtain the electrons to transform into Ni on the cathode's surface, plus having more energy to conquer the resistances present in every perspective of the electrochemical system through the application of negative electrical potentials, giving a more conducive environment for electrowinning.

In future work, the applied potential in the experiment needs to be reduced slowly with time intervals, changing from −0.5 V to −3.5 V, which can always obtain the silver deposition. To do so, it is better to have a separated potential supplier and potential measuring and recording machine in the experiment to avoid heavy burden of the equipment, so that the electrochemical system can just extract the required amount of energy from the potential supplier automatically. Otherwise, the potentiostat and other components of the electrochemical system, such as the reference electrode, need to have regular maintenance to ensure that it give more steady and accurate readings while doing strenuous task of reducing the applied potential.

4. CONCLUSION

Based on this investigation, graphite cathode exhibits the highest Ni^{2+} recovery rate (56.74%) compared to nickel cathode (55.90%) and AISI 304 stainless steel cathode (50.66%) at settings of 0.5 V, pH 5, and 3 hours of contact time at ambient environmental conditions. Graphite has the maximum current efficiency at 39.57%, followed by nickel at 24.35% and AISI 304 stainless steel at 6.09%. This indicates that the current efficiency of materials is directly proportional to the nickel recovery levels. By utilizing the Analytical Hierarchy Process and the Technique for Order of Preference by Similarity to Ideal Solution (AHP-TOPSIS) combination selection method, it has been determined that nickel cathode is the most effective commercial cathode material type for maximising nickel recovery. Maximum nickel recovery of 70.18% is achieved with the ideal electrowinning conditions of a nickel cathode at pH 6, 0.5 V, and 1 hour. Scanning electron microscopy (SEM) and energy-dispersive X-ray (EDX) analysis reveal that impurities consisting of sodium crystals are deposited together with dendritic nickel on a uniformly distributed microporous rough surfaced graphite cathode. Nickel cathodes exhibit discontinuous multicrystalline layers with grains and nickel boundaries. On the other hand, AISI 304 stainless steel cathodes have a smooth layer of small grain sizes with a large grain boundary network and the lowest nickel content among all the cathodes. The present work has identified kinetic interactions in the Nernst, Tafel, Butler Volmer, and Anson equations using cyclic and linear sweep voltammetry.

ACKNOWLEDGMENTS

The author would like to express heartfelt gratitude to L'Oréal-UNESCO For Women In Science (FWIS) research grant (9008-00018) for its valuable financial support, which significantly contributed to the success of this study.

REFERENCES

[1] "About Nickel," *Nickel Institute*. https://nickelinstitute.org/en/nickel-applications/#04-first-use-nickel (accessed Sep. 07, 2024).

[2] "A Global Pathway to Keep the 1.5°C Goal in Reach," *Net Zero Roadmap*, Sep. 2023. https://www.iea.org/reports/net-zero-roadmap-a-global-pathway-to-keep-the-15-0c-goal-in-reach (accessed Sep. 07, 2024).

[3] K. S. Nivedhitha *et al.*, "From nickel–metal hydride batteries to advanced engines: A comprehensive review of hydrogen's role in the future energy landscape," International Journal of Hydrogen Energy, vol. 82, pp. 1015–1038, 2024, doi: 10.1016/j.ijhydene.2024.07.271.

[4] R. Emanuele *et al.*, "Nickel release from 316L stainless steel following a Ni-free electroplating cycle," *Heliyon,* vol. 10, no. 17, p. e37125, 2024, doi: 10.1016/j.heliyon.2024.e37125.

[5] A. F. M. Salcedo, F. C. Ballesteros, A. C. Vilando, and M.-C. Lu, "Nickel recovery from synthetic Watts bath electroplating wastewater by homogeneous fluidized bed granulation process," *Separation and Purification Technology*, vol. 169, pp. 128–136, 2016, doi: 10.1016/j.seppur.2016.06.010.

[6] S. Jerroumi, M. Amarine, H. Nour, B. Lekhlif, and J. E. Jamal, "Removal of nickel through sulfide precipitation and characterization of electroplating wastewater sludge," *Water Quality Research Journal*, vol. 55, no. 4, pp. 345–357, 2020, doi: 10.2166/wqrj.2020.116.

[7] A. Pohl, "Removal of Heavy Metal Ions from Water and Wastewaters by Sulfur-Containing Precipitation Agents," *Water Air & Soil Pollution*, vol. 231, no. 10, 2020, doi: 10.1007/s11270-020-04863-w.

[8] J. Wang, Y. Zhang, L. Yu, K. Cui, T. Fu, and H. Mao, "Effective separation and recovery of valuable metals from waste Ni-based batteries: A comprehensive review," *Chemical Engineering Journal,* vol. 439, p. 135767, 2022, doi: 10.1016/j.cej.2022.135767.

[9] A. Fathima, J. Y. B. Tang, A. Giannis, I. M. S. K. Ilankoon, and M. N. Chong, "Catalysing electrowinning of copper from E-waste: A critical review," *Chemosphere*, vol. 298, p. 134340, 2022, doi: 10.1016/j.chemosphere.2022.134340.

[10] U. F. Md. Ali, "Electrochemical Separation and Purification of Metals from Waste Electrical and Electronic Equipment (WEEE)," PhD Dissertation, Imperial College, London., 2011.

[11] M. Baraniak *et al.*, "From nickel waste solution to hydrogen storage alloys – An excellent example of circular economy implementation," *Separation and Purification Technology*, vol. 328, p. 125063, 2023, doi: 10.1016/j.seppur.2023.125063.

[12] Z. Zhang, J. M. Werner, and M. L. Free, "Modeling Nickel Electrowinning with Electrode Diaphragms Based on Nernst-Plank Equation and a Volume Force Form of Darcy's Law," *Journal of the Electrochemical Society*, vol. 166, no. 4, pp. D120–D130, 2019, doi: 10.1149/2.0281904jes.

[13] A. Kazem-Ghamsari and H. Abdollahi, "Electrowinning of Nickel and Cobalt from Non-circulated Sulfate Electrolyte," *Transactions of the Indian Institute of Metals*, vol. 75, no. 5, pp. 1141–1151, 2022, doi: 10.1007/s12666-021-02457-6.

[14] P. Laokhen, N. Ma-Ud, T. Yingnakorn, T. Patcharawit, and S. Khumkoa, "Recovery of nickel from spent electroplating solution by hydrometallurgical and electrometallurgical process," *Journal of Metals*

Materials and Minerals, vol. 32, no. 2, pp. 95–100, 2022, doi: 10.55713/jmmm.v32i2.1253.

[15] Q. Gao *et al.*, "Facile electrodeposition of corrosion-resistant superhydrophobic Ni-plated stainless-steel mesh for oil–water separation," *Materials Today Communications*, vol. 37, p. 107032, 2023, doi: 10.1016/j.mtcomm.2023.107032.

[16] T. Pérez et al., "Simulations of fluid flow, mass transport and current distribution in a parallel plate flow cell during nickel electrodeposition," *Journal of Electroanalytical Chemistry*, vol. 873, p. 114359, 2020, doi: 10.1016/j.jelechem.2020.114359.

[17] C. Wang, T. Li, G. Yu, and S. Deng, "Removal of low concentrations of nickel ions in electroplating wastewater by combination of electrodialysis and electrodeposition," *Chemosphere*, vol. 263, p. 128208, 2020, doi: 10.1016/j.chemosphere.2020.128208.

[18] A. K. Chaurasia, H. Goyal, and P. Mondal, "Hydrogen gas production with Ni, Ni–Co and Ni–Co–P electrodeposits as potential cathode catalyst by microbial electrolysis cells," *International Journal of Hydrogen Energy*, vol. 45, no. 36, pp. 18250–18265, 2019, doi: 10.1016/j.ijhydene.2019.07.175.

[19] Sudibyo *et al.*, "Nickel recovery from electrocoagulation sludge of hydrometallurgy wastewater using electrowinning," *AIP Conference Proceedings*, vol. 2232, no. 1, p. 020008, Apr. 2020, doi: 10.1063/5.0001929

[20] C. Stinn and A. Allanore, "Selective Sulfidation and Electrowinning of Nickel and Cobalt for Lithium Ion Battery Recycling," in *Ni-Co 2021: The 5th International Symposium on Nickel and Cobalt*, C. Anderson, G. Goodall, S. Gostu, D. Gregurek, M. Lundström, C. Meskers, S. Nicol, E. Peuraniemi, F. Tesfaye, P. K. Tripathy, S. Wang, and Y. Zhang, Eds., Cham: Springer International Publishing, 2021, pp. 99–110, doi: 10.1007/978-3-030-65647-8_7.

[21] T. Li *et al.*, "Recovery of Ni(II) from real electroplating wastewater using fixed-bed resin adsorption and subsequent electrodeposition," *Frontiers of Environmental Science & Engineering*, vol. 13, no. 6, 2019, doi: 10.1007/s11783-019-1175-7.

[22] L. Schoeman, E. N. Nsiengani, K. C. Sole, and R. Sandenbergh, "Effect of aluminium on polarisation parameters and deposit characteristics in typical nickel sulfate electrolyte for electrowinning applications," *Hydrometallurgy*, vol. 194, p. 105332, 2020, doi: 10.1016/j.hydromet.2020.105332.

[23] C. Sherwin, S. Bhat, and S. P Hebbar, "Effects of Current Density on Surface Morphology and Coating Thickness of Nickel Plating on Copper Surface," *Turkish Journal of Computer and Mathematics Education (TURCOMAT)*, vol. 12, no. 10, pp. 79–83, 2021.

[24] M. Próchniak and M. Grdeń, "Electrochemical deposition of nickel from aqueous electrolytic baths prepared by dissolution of metallic powder," *Journal of Solid State Electrochemistry*, vol. 26, no. 2, pp. 431–447, 2021, doi: 10.1007/s10008-021-05084-9.

[25] I. Korolev, K. Yliniemi, M. Lindgren, L. Carpén, and M. Lundström, "Performance-Based Selection of the Cathode Material for the Electrodeposition-Redox Replacement Process of Gold Recovery from Chloride Solutions," *Metallurgical and Materials Transactions B*, vol. 52, no. 5, pp. 3107–3119, 2021, doi: 10.1007/s11663-021-02239-x.

[26] J. Tang, Y. Bian, S. Jin, D. Sun, and Z. J. Ren, "Cathode Material Development in the Past Decade for H_2 Production from Microbial Electrolysis Cells," *ACS Environmental Au*, vol. 2, no. 1, pp. 20–29, 2021, doi: 10.1021/acsenvironau.1c00021.

[27] R. G. Compton, E. Laborda, and K. R. Ward, *Understanding voltammetry*. Imperial College Press, 2014. doi: 10.1142/p910.

[28] M. A. López-Mata *et al.*, "Physicochemical and Antioxidant Properties of Chitosan Films Incorporated with Cinnamon Oil," *International Journal of Polymer Science*, vol. 2015, pp. 1–8, 2015, doi: 10.1155/2015/974506.

[29] K. Li, Y. Li, L. Wang, L. Yang, and B. Ye, "Study the voltammetric behavior of 10-Hydroxycamptothecin and its sensitive determination at electrochemically reduced graphene oxide modified glassy carbon electrode," *Arabian Journal of Chemistry*, vol. 12, no. 8, pp. 2732–2739, 2015, doi: 10.1016/j.arabjc.2015.05.014.

[30] N. Z. Zulkurnai, Y. M. Hua, U. F. M. Ali, M. I. H. M. Dzahir, N. Ibrahim, and F. M. Zuki, "Optimization of Nickel Electrowinning from Simulated Watts Bath of Electronics Industrial Waste," in *Emerging Technologies for Future Sustainability*, H. Shukor, H. N. A. Halim, H. L. Ong, B.-B. Lee, and M. H. M. Pisal, Eds., Singapore: Springer Nature Singapore, 2023, pp. 311–323, doi: 10.1007/978-981-99-1695-5_27.

[31] R. Leiva-García, M. J. Muñoz-Portero, and J. García-Antón, "Influence of sensitisation on the corrosion behaviour of alloy 926 (UNS N08926) in concentrated aqueous lithium bromide solutions at different temperatures," *International Journal of Electrochemical Science*, vol. 6, no. 2, pp. 442–460, 2011, doi: 10.1016/s1452-3981(23)15007-3.

[32] S. M. Peshcherova, E. B. Yakimov, A. I. Nepomnyashchikh, L. A. Pavlova, and O. V. Feklisova, "Recombination activity of interfaces in multicrystalline silicon," *Semiconductors*, vol. 49, no. 6, pp. 724–728, 2015, doi: 10.1134/s1063782615060196.

[33] A. Gupta and C. Srivastava, "Low-temperature Sn electrodeposition: Texture evolution, grain boundary constitution and corrosion behavior," *Surface and Coatings Technology*, vol. 425, p. 127709, 2021, doi: 10.1016/j.surfcoat.2021.127709.

[34] A. A. Giwa, A. T. Adetunji, and F. Wewers, "Assessment of Negro pepper (Xylopia aethiopica) fruit extracts as corrosion inhibitors for Mild steel," *Journal of Materials and Environmental Science*, vol. 11, no. 7, pp. 1100–1111, 2020.

[35] Y. Chu, G. Yu, B. Hu, Q. Dong, J. Zhang, and X. Zhang, "Effect of hypophosphite on electrodeposition of graphite@copper powders," *Advanced Powder Technology*, vol. 25, no. 2, pp. 477–482, 2014., doi: 10.1016/j.apt.2013.07.003.

[36] A. Karimzadeh, M. Aliofkhazraei, and F. C. Walsh, "A review of electrodeposited Ni-Co alloy and composite

coatings: Microstructure, properties and applications," *Surface and Coatings Technology*, vol. 372, pp. 463–498, 2019, doi: 10.1016/j.surfcoat. 2019.04.079.

[37] M. Ismon *et al.*, "Pitting Hole Evaluation by Active Infrared Thermography in Stainless Steel 304," *Journal of Advanced Research in Fluid Mechanics and Thermal Sciences*, vol. 68, no. 1, pp. 114–124, 2024.

[38] H. Jäger and W. Frohs, Eds., *Industrial Carbon and Graphite Materials: Production and Applications,* Wiley, 2021.

[39] M. Jaganmohan, "Supply of nickel worldwide from 2019 to 2021, with estimated figures for 2022 and 2023," *Statista*, 2024. https://www.statista. com/statistics/1245590/nickel-supply-worldwide/ (accessed Dec. 12, 2024).

[40] "World Steel in Figures 2023," *Worldsteel Association*, 2023. https://worldsteel.org/data/ world-steel-in-figures/world-steel-in-figures-2023/ (accessed Dec. 12, 2024).

[41] "What is 304 Stainless Steel?," *BorTec*, 2022. https://bortec-group.com/glossary/304-steel/ #:~:text=304%20is%20characterized%20by%20a,in%20the%20amount%20of%20carbon (accessed Dec. 12, 2024).

[42] M. Jaganmohan, "Mine production of graphite worldwide from 2010 to 2023 (in 1,000 metric tons)," *Statista,* 2024. https://www.statista.com/ statistics/1005851/global-graphite-production/ (accessed Dec. 12, 2024).

[43] G. Kelly, "Apple Confirms It Knew About iPhone 'Bendgate'," Forbes, May 24, 2018. https://www. forbes.com/sites/gordonkelly/2018/05/24/apple-iphone-problem-iphone-6-iphone-6-plus-bend-touchscreen/ (accessed Dec. 12, 2024).

[44] C. Stinn and A. Allanore, "Estimating the capital costs of electrowinning processes," *Electrochemical Society Interface*, vol. 29, no. 2, pp. 44–49, 2020, doi: 10.1149/2.f06202if.

[45] Y. Guo, C. Zhao, X. Qin, and J. Zhang, "Prediction and Analysis of Wuxi Stainless Steel Market Price Based on ARIMA-BP Neural Network Combination Model," *International Journal of Managerial Studies and Research*, vol. 10, no. 7, pp. 40–52, 2022, doi: 10.20431/2349-0349.1007005.

[46] M. C. R. Muhammad, "Nickel Price Projection Using Multivariate Regression Method and Investment Feasibility Analysis of Nickel Mining in Indonesia with Sensitivity Analysis and Monte Carlo," *International Journal of Current Science Research and Review*., vol. 07, no. 03, pp. 1728–1737, 2024, doi: 10.47191/ijcsrr/v7-i3-34.

[47] B. G. Abraham and R. Chetty, "Influence of electrodeposition techniques and parameters towards the deposition of Pt electrocatalysts for methanol oxidation," *Journal Applied Electrochemistry*., vol. 51, pp. 503–520, 2021, doi: 10.1007/s10800-020-01510-4.

[48] Pine Research Instrumentation, "Exploring Faraday's Law Using Inexpensive Screen-Printed Electrodes," *Pine Research Institute*, USA, 2019.

[49] M. H. Salmani, M. Abedi, S. A. Mozaffari, A. H. Mahvi, A. Sheibani, and M. Jalili, "Simultaneous reduction and adsorption of arsenite anions by green synthesis of iron nanoparticles using pomegranate peel extract," *Journal Environment Science and Engineering*., vol. 19, no. 1, pp. 603–612, 2021, doi: 10.1007/s40201-021-00631-y.

[50] L. M. Cursaru, A. G. Plaiasu, C. M. Ducu, R. M. Piticescu, and I. A. Tudor, "Carbon Nanotube/Polyaniline Composite Films Prepared by Hydrothermal-Electrochemical Method for Biosensor Applications," in *2018 International Semiconductor Conference (CAS)*, IEEE, 2018, pp. 249–252, doi: 10.1109/ SMICND.2018.8539793.

[51] W. T. Tee, N. Y. L. Loh, B. Y. Z. Hiew, S. Hanson, S. Thangalazhy-Gopakumar, S. Gan, and L. Y. Lee, "Effective remediation of lead(II) wastewater by Parkia speciosa pod biosorption: Box-Behnken design optimisation and adsorption performance evaluation," *Biochemical Engineering Journal*, vol. 187, pp. 108629, 2022, doi: 10.1016/j.bej.2022. 108629.

[52] Z. Hou, T. Liu, M. U. Tahir, S. Ahmad, X. Shao, C. Yang, B. He, and X. Su, "Facile conversion of nickel-containing electroplating sludge into nickel-based multilevel nano-material for high-performance pseudocapacitors," *Applied Surface Science*, vol. 538, pp. 147978, 2021, doi: 10.1016/j.apsusc.2020. 147978.

[53] M. Shamsuddin, *Physical Chemistry of Metallurgical Processes*, Springer Nat. Switzerland, 2021.

[54] H. Dawson, "Friction Stir Welding of ODS Steels for Future Generation Nuclear Reactors," Ph.D. dissertation, University of Manchester, 2017.

[55] C. Satyanarayanaraju and C. V. Krishnamurthy, "Charge migration model for the impedance response of DI water," *AIP Advance*, vol. 9, no. 3, p. 035141, 2019, doi: 10.1063/1.5078709.